

Recent Estimation Techniques of Vehicle-Road-Pedestrian States for Traffic Safety: Comprehensive Review and Future Perspectives

Cheng Tian⁴¹, Graduate Student Member, IEEE, Chao Huang⁴¹, Senior Member, IEEE, Yan Wang⁶, Member, IEEE, Edward Chung⁶, Anh-Tu Nguyen⁶, Senior Member, IEEE, Pak Kin Wong⁶, Wei Nie⁶, Fellow, IEEE, Abbas Jamalipour⁶, Fellow, IEEE, Kai Lie⁶, Senior Member, IEEE, and Hailong Huang⁶, Senior Member, IEEE

*Abstract-*Accurate and real-time acquisition of vehicular system dynamic states, road surface conditions, and motion states of surrounding participants is crucial for the safety, passenger comfort, and operational efficiency of autonomous vehicles (AVs) and connected automated vehicles (CAVs). In recent years, a significant amount of research has contributed to the field of state estimation for vehicles, roads, and pedestrians. From the systemwide perspective of intelligent transportation systems to a focused view on "vehicle-road-pedestrian", this survey aims to provide a comprehensive review and summary of recent state estimation techniques for vehicle motion, road surface, and pedestrian motion. A thorough analysis of the reviewed literature, relevant datasets, evaluation metrics, and experimental platforms in this field is also conducted. Finally, existing challenges and future research directions about methods and performance evaluation are further discussed. This survey is expected to contribute to the advancement of research in dynamic state estimation of vehicle-road-pedestrian, thereby facilitating the development of efficient and safe intelligent transportation systems.

Received 11 March 2024; revised 15 August 2024 and 13 November 2024; accepted 9 December 2024. Date of publication 25 December 2024; date of current version 3 March 2025. This work was supported by the Smart Traffic Fund Project under Grant PSRI/47/2209/PR. The Associate Editor for this article was L. Li. (*Corresponding author: Haitong Huang*)

Cheng Tian and Hailong Huang are with the Department of Aeronautical and Aviation Engineering, The Hong Kong Polytechnic University, Hong Kong, SAR, China (e-mail: cheng7.tian@connect.polyu.hk; hailong.huang@polyu.edu.hk).

Chao Huang and Yan Wang are with the Department of Industrial and Systems Engineering, The Hong Kong Polytechnic University, Hong Kong, SAR, China (e-mail: hchao.huang@polyu.edu.hk; yanjack.wang@polyu.edu.hk).

Edward Chung is with the Department of Electrical and Electronic Engineering, The Hong Kong Polytechnic University, Hong Kong, SAR, China (e-mail: edward.cs.chung@polyu.edu.hk).

Anh-Tu Nguyen is with the LAMIIH Laboratory, UMR CNRS 8201, and INSA Hauts-de-France, Université Polytechnique Hauts-de-France, 59300 Valenciennes, France (e-mail: tnguyen@uphf.fr).

Pak Kin Wong is with the Department of Electromechanical Engineering, University of Macau, Macau, China (e-mail: fstpkw@um.edu.mo).

Wei Ni is with the Data61, Commonwealth Scientific and Industrial Research Organization, Sydney, NSW 2122, Australia (e-mail: wei.ni@data61.csiro.au).

Abbas Jamalipour is with the School of Electrical and Computer Engineering, The University of Sydney, Sydney, NSW 2006, Australia (e-mail: ajamalipour@ieee.org).

Kai Li is with the Department of Engineering, University of Cambridge, CB3 OFA Cambridge, U.K., and also with the Real-Time and Embedded Computing Systems Research Centre (CISTER), 4249-015 Porto, Portugal (e-mail: kaili@ieee.org).

Digital Object Identifier 10.1109/TITS.2024.3517162

Index Terms- Vehicle state estimation, road surface state estimation, pedestrian motion state estimation, vehicle-road-pedestrian, intelligent transportation systems.

NOMENCLATURE

| | |
|------|-------------------------------------|
| ANN | Artificial Neural Network. |
| AVs | Autonomous Vehicles, |
| CAVs | Connected and Automated Vehicles, |
| CKF | Cubature Kalman Filter. |
| CNN | Convolutional Neural Network. |
| DNN | Deep Neural Network. |
| DoF | Degree of Freedom, |
| EKF | Extended Kalman Filter. |
| GNSS | Global Navigation Satellite System, |
| HIL | Hardware in Loop, |
| IMM | Interactive Multiple Model, |
| IMU | Inertial Measurement Unit. |
| KF | Kalman Filter. |
| LSTM | Long Short-Term Memory. |
| MF | Magic Formula tire model, |
| ML | Machine Learning. |
| NN | Neural Network. |
| PF | Particle Filter. |
| RNN | Recurrent Neural Network. |
| TRFC | Tire-Road Friction Coefficient. |
| UKF | Unscented Kalman Filter. |
| V2I | Vehicle to Infrastructure. |
| V2N | Vehicle to Network. |
| V2V | Vehicle to Vehicle. |
| V2X | Vehicle to Everything. |

I. INTRODUCTION

TRAFFIC accidents continue to be a major global concern, resulting in significant loss of life, injuries, and economic damage. In recent years, the development of autonomous vehicles (AVs) and connected and automated vehicles (CAVs) has shown great potential for reducing human-related traffic accidents. These techniques offer innovative solutions that improve traffic safety and overall traffic efficiency [1].

AVs and CAVs are important paradigms and components of future intelligent transportation systems (ITS) [2]. The

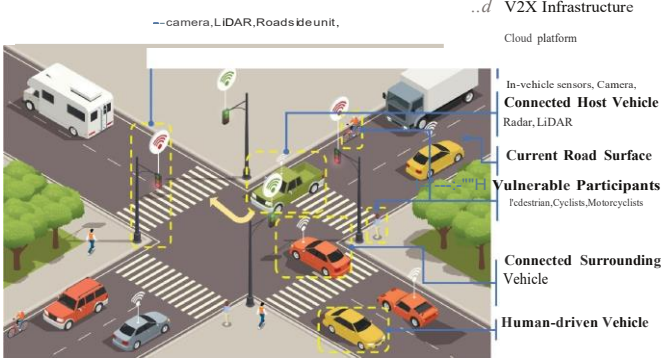


Fig. 1. Illustration of intelligent transportation systems.

schematic diagram of intelligent transportation systems is shown in Fig. L The key components of intelligent transportation systems are as follows:

Vehicles: The vehicles mainly include AVs, CAVs, human-driven vehicles, and connected human-driven vehicles. The coexistence of AVs and human-driven vehicles in a mixed traffic mode is considered the most promising composition model for the future of intelligent transportation systems [3]. **Vulnerable Participants:** Vulnerable participants (i.e., vulnerable road users) primarily consist of pedestrians, cyclists, and motorcycle riders [4]. Due to the significant variability in pedestrian motion behavior, they are more prone to injuries. Therefore, the relevant literature about the estimation of pedestrian motion states is selected to be reviewed in this survey. **Road Surface:** Road surface state information usually includes road friction, road bank, road slope, and road unevenness. Considering that road friction and road unevenness can directly affect the vehicle chassis stability and passenger comfort, further reviews of the research on road friction and road unevenness pre-identification are needed. The estimation results can be used for road surface condition monitoring and early warning systems.

Roadside Infrastructure: Intelligent roadside infrastructure units can detect traffic conditions in advance and have a wider field of view compared to the ego-vehicle perspective in occlusion situations. The perception sensors equipped on the roadside infrastructure mainly include roadside lidar and roadside cameras, which are mainly responsible for detecting and sensing status information, such as the location, type, speed, and heading angle of traffic participants. The roadside cloud computing platform is responsible for sensing the area. The data collected by the facilities is quickly analyzed and calculated, and roadside facilities are coordinated to provide auxiliary information to connected vehicles [5].

Communication Devices: Communication devices in intelligent transportation systems include the global navigation satellite system (GNSS), dedicated short-range communications (DSRC), and cellular networks. GNSS provides accurate vehicle position and velocity, enabling high-precision time synchronization for data transmission. DSRC facilitates V2X low-latency communication, allowing real-time information exchange between vehicles and infrastructure. The 5G cellular network offers broader signal coverage and larger bandwidth but introduces higher communication delays, making it suitable for services like vehicle navigation [6].

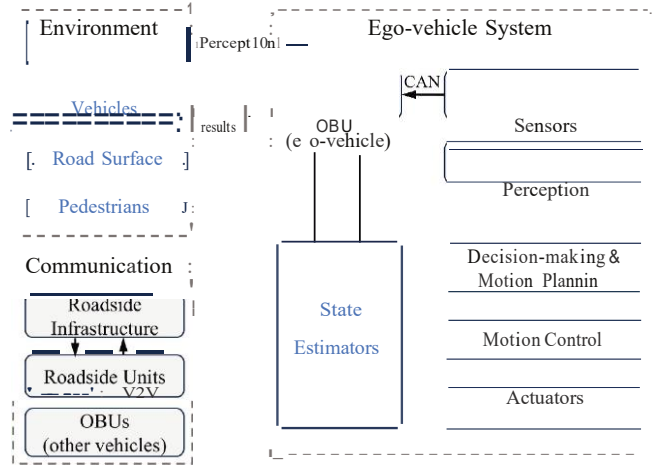


Fig. 2. General architecture of a CAV system. OBU: on-board unit.

In autonomous driving systems, autonomous driving levels are usually classified using the SAE international autonomous driving level definition (SAE J3016), which divides autonomous driving systems into six levels [1]. The electronic stability program (ESP) that performs instantaneous intervention in vehicle motion states belongs to LO (No Driving Automation) and has made significant contributions to vehicle driving safety, such as tracking control systems (TCS) and anti-lock braking systems (ABS) [7]. Advanced driver assistance systems (ADAS), which mainly fall under the L1 (Driver Assistance) or L2 (Partial Driving Automation) levels of automation, serve as foundational technological features for AVs. ADAS utilizes perception sensors to detect the surrounding environment, assisting drivers in avoiding traffic accidents or reducing driving fatigue. These systems can even actively control the longitudinal and lateral motion of the vehicle to improve driving safety and comfort [8], [9], such as adaptive cruise control (ACC), lane keeping assist (LKA), and driver state monitoring system [10], [11]. In addition to AV technologies, CAVs that integrate Vehicle-to-Vehicle (V2V), Vehicle-to-Infrastructure (V2I), and Vehicle-to-Everything (V2X) communications can emerge as a promising technology. V2X technology enables real-time sensor data communication between connected vehicles and the data exchange between connected vehicles and roadside infrastructure, which can reduce limited vision spots and uncertainties in driving within complex traffic environments [6].

A. Scope

The general architecture of a CAV system is presented in Fig. 2. This survey focuses on recent estimation techniques of vehicle sideslip angle, road surface states, and motion states of surrounding vehicles and pedestrians. It is particularly important in the sense that precise acquisition of vehicle body states, tire-road interaction, and pedestrian state information is vital for decision-making, motion planning, and motion control systems in AVs and CAVs [12]. Typical dynamic states of the vehicle body include longitudinal and lateral velocity, yaw rate, vehicle rolling angle, vehicle pitch angle, and the vehicle sideslip angle. Among these states, the vehicle sideslip angle is relatively more important as a comprehensive vehicle state,

which consists of longitudinal velocity and lateral velocity information. Since the longitudinal velocity is much easier to estimate than the lateral velocity [13], the estimation of vehicle sideslip angle and lateral velocity receives strong attention in this survey. Road surface state estimation is more concerned with the estimation of the following states: tire-road forces, tire-road friction coefficient (TRFC), road unevenness, road bank angle, and road slope angle. It is worth noting that TRFC is defined as the ratio of maximum tire friction force to tire normal force. TRFC is an essential state to characterize the adhesion ability of the tire to the road surface. Road unevenness mainly affects the vertical dynamics of the chassis and reduces passenger comfort. Severe road unevenness may even threaten the driving safety of AVs and CAVs. In addition, compared with other road parameters such as road bank and road slope, the time variability of TRFC and road unevenness is stronger. Considering the cost and generalization, this survey does not discuss the research of TRFC estimation based on intelligent tires. However, some industrial solutions for tire force estimation available in the market are briefly reviewed. The unpredictable motion behavior of pedestrians further complicates the safe and efficient operation of AVs and CAVs. Nonetheless, limitations in existing sensors and cost factors make it challenging to directly measure key states like vehicle sideslip angle, TRFC, road unevenness, and pedestrian motion states [14], [15]. As a result, rapid and robust estimation methods for the above key states received significant attention in both academic and industrial fields.

B. Review Methodology

This paper used a strict systematic literature sample method that involved sorting and screening relevant articles published between 2019 and 2023. In addition, before 2019, relevant articles were selected to provide background information or explain certain concepts. Specifically, the search was initially focused on the publication years between 2019 and 2023, and the keywords "vehicle sideslip angle estimation", "vehicle lateral velocity estimation", "tire-road forces estimation", "tire-road friction estimation", and "road unevenness, road pothole detection" were separately used to conduct searches in the *IEEE Xplore* database and the *Scopus* database. It is important to note that searching for "surrounding participant state estimation" directly in the database would yield irrelevant literature results. To find applicable literature on the topic of motion states of surrounding vehicles and pedestrians, this study used terms, such as "preceding vehicle state estimation", "multi-vehicle tracking", and "pedestrian tracking". TABLE I shows the number of references. After manually filtering the identified literature using Prisma systematic review criteria [16], title, abstract, and full-text assessments were performed. Additionally, lecture notes, theses, book chapters, reports, non-English literature, and low-representative works were removed. Finally, 190 references were reviewed in depth.

As shown in Fig. 3, approximately 89% of the publications were published in journals and 11% in conference proceedings. Additionally, the publications considered in this paper were categorized based on the Journal Citation Reports (JCR)

TABLE I
NUMBER OF REFERENCES FOUND AT THE INITIAL STAGE

| Keywords | IEEE Xplore | Scopus |
|---|-------------|--------|
| "vehicle sideslip angle estimation" | 236 | 239 |
| "vehicle lateral velocity estimation" | 258 | 205 |
| "tire-road friction estimation" | 54 | 132 |
| "road unevenness, road pothole detection" | 320 | 785 |
| "tire-road forces estimation" | 62 | 98 |
| "preceding vehicle state estimation" | 30 | 32 |
| "multi-vehicle tracking" | 113 | 178 |
| "pedestrian tracking" | 1909 | 1799 |

TABLE II
COMPARISON OF THIS SURVEY WITH OTHER RELATED SURVEYS

| Survey Year | Ego | Road | STPS | V2X | Met. | Test | Cit.* | Ref. | Future | scope |
|-------------|------|------|------|-----|------|------|-------|------|-------------------|-------|
| [17] | 2018 |)< |)< |)< |)< |)< | 141 | 97 | <i>CIRN</i> | |
| [14] | 2019 |)< |)< |)< |)< |)< | 79 | 139 | <i>MIUN</i> | |
| [18] | 2019 | |)< |)< |)< |)< | 117 | 131 | C/M | |
| [19] | 2021 |)< |)< | |)< |)< | 930 | 214 | M | |
| [15] | 2021 |)< |)< | |)< |)< | 85 | 147 | R | |
| [4] | 2022 |)< |)< | | |)< | 47 | 360 | <i>MN</i> | |
| [20] | 2022 |)< | |)< |)< |)< | 52 | 117 | <i>MN</i> | |
| [13] | 2023 | |)< |)< | |)< | 20 | 296 | M | |
| [21] | 2023 | | | |)< |)< | 5 | 201 | <i>CIRN</i> | |
| Ours | | | | | |)< | | 230 | <i>MIFIP/R/EN</i> | |

¹ Ego: Ego-vehicle state; Road: Road Surface; Test: Test Platform; STPS: surrounding traffic participant states; Met.: metrics; Ref.: total cited references; : applicable; J<: not applicable. In "Future scope", C: coupling dynamics; F: fault-tolerant; M: multisensor-based; P: public datasets; R: robust and real-time; E: effective test platform; V: V2X-based.

² Cit.: Citation (source: Google Scholar), *Date: 8-Mar-2024

category of Web of Science. The top THREE categories, in terms of percentage, are as follows: "ENGINEERING, MECHANICAL" (27.88%), "ENGINEERING, ELECTRICAL & ELECTRONIC" (25.45%), "INSTRUMENTS & INSTRUMENTATION" (14.55%). This paper offers a more comprehensive summary of recent state estimation techniques for vehicle-road-pedestrian of ITS, addressing aspects not fully covered in existing surveys. Details of the specific comparisons are presented in TABLE II.

C. Contributions

The overall framework of this survey is shown in Fig. 4. In this study, we offer a general perspective on ITS and focus on a specific perspective of "vehicle-road-pedestrian" triad. The contributions of this paper can be summarized as follows:

- 1) Recent typical and state-of-the-art dynamic state estimation methods for vehicle-road-pedestrian are thoroughly reviewed. The applicability, pros, and cons of various approaches are analyzed in detail.
- 2) Unlike the previous surveys [4], [13], [14], [17], [18], [20], [21], evaluation metrics and experiment platforms for the typical estimation methods are comprehensively summarized.
- 3) Existing research gaps and challenges are identified, including model uncertainty caused by tire wear or highly dynamic nonlinear conditions, performance degradation due to signal dropout or cyberattacks, and lack of public datasets and effective test platforms.

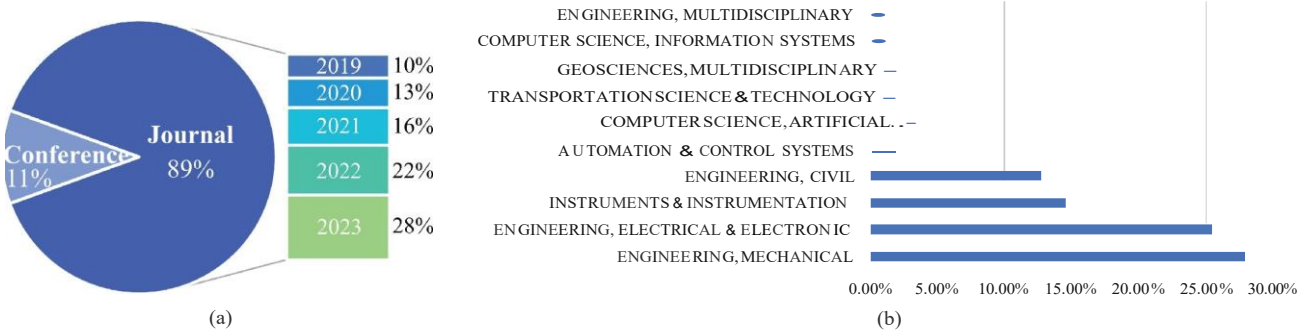


Fig. 3. Distribution of the reviewed references. (a) The type of the reviewed references. (b) JCR category of reviewed references.

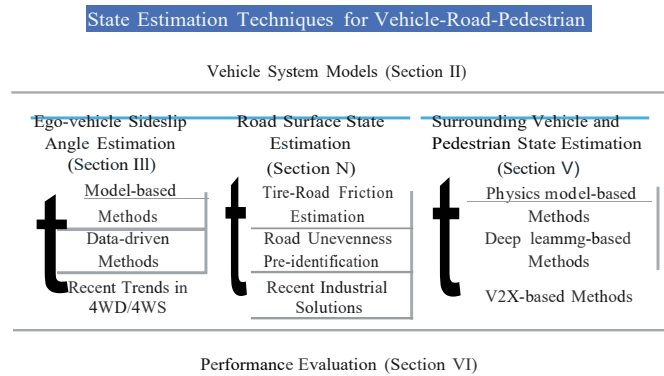


Fig. 4. Overall framework of this survey. 4WD/4WS: four-wheel drive and four-wheel steering platforms.

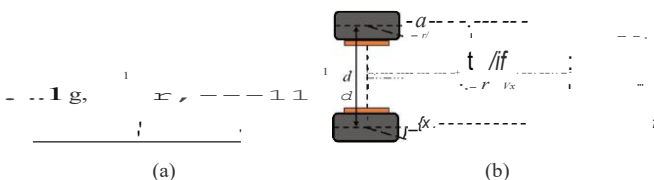


Fig. 5. Schematic diagram of common vehicle models. (a) Single-track vehicle model. (b) Double-track vehicle model.

4) Future research directions are also outlined, such as multi-sensor fusion, fault-tolerance, and effective evaluation.

The paper is organized as follows: Section II introduces typical vehicle and tire models for state estimation algorithms. Sections III, IV, and V comprehensively review recent state estimation methods for vehicle sideslip angle, road surface states, and motion states of surrounding vehicles and pedestrians, respectively. Section VI summarizes datasets, evaluation metrics, and experimental platforms related to dynamic state estimation. Section VII discusses current challenges and future directions, and Section VIII concludes the key findings.

II. VEHICLE SYSTEM MODELS

The modeling of the vehicle and the tire-road forces is crucial for developing estimation algorithms that reconstruct essential information about the ego-vehicle and its interaction with the roads. The vehicle and tire-road models commonly used in ITS are summarized in TABLE III and TABLE IV, respectively.

A. Vehicle Models

As shown in Fig. 5a, the single-track vehicle model, also known as the bicycle model, is considered by merging the left and right wheels into a single wheel. The single-track vehicle model can be further classified into kinematic and dynamic models.

The kinematic single-track model is established on the

low speeds (less than 5 m/s). This model is only valid when the lateral acceleration can be approximately disregarded. Consequently, the model performance may significantly degrade during high-speed cornering, and it fails to investigate the load transfer between wheels due to the lack of consideration for tire forces.

Due to the tire slip angle that occurs at high vehicle speeds, the kinematic model becomes inadequate. The dynamic single-track model takes into account dynamic elements such as mass, inertia, force, and moment, thereby providing an accurate depiction of vehicular motion [1]. Depending on whether the longitudinal degree of freedom (DoF) is considered, the dynamic single-track model can be further divided into the 2-DoF dynamic model and the 3-DoF dynamic model, both of which include the lateral and yaw motion of the vehicle. It is worth noting that the dynamic single-track model can not only consider the complete planar motion of the rigid body (longitudinal, lateral, and yaw motion) but also can incorporate load transfer between the front and rear axles. It can effectively combine longitudinal dynamics and tire models in most scenarios. However, it cannot account for the lateral load transfer during high-speed cornering.

As shown in Fig. 5b, the dynamic double-track model includes 7 degrees of freedom such as longitudinal motion, lateral motion, yaw motion of the vehicle on the plane, and the rotation of the four wheels. Compared to the dynamic single-track model, the dynamic double-track model provides a more accurate description of vehicle motion by considering both longitudinal and lateral load transfer. It also takes into account the longitudinal tire forces, lateral tire forces, and normal tire forces of all four wheels simultaneously. However, it requires higher computational resources.

B. Tire Models

A tire dynamics model is a dynamics model that describes the steady-state motion of the tire. Currently, the tire steady-state model can be divided into empirical models,

TABLE III
SUMMARY OF COMMON VEHICLE MODELS FOR STATE ESTIMATION METHODS OF VEHICLE-ROAD-PEDESTRIAN

| Vehicle models | Motion states | Advantages | Disadvantages | Scenarios |
|------------------------|----------------------------------|---|--|--|
| Kinematic single-track | $(X, Y), \delta\theta, v_x, v_y$ | Low computational burden | 1) Not considering the impact of tire forces on the vehicle body; 2) Degradation during high-speed cornering | 1) Available in scenarios with low speed (< 5 m/s) and almost no lateral acceleration; 2) Capable of being used in vehicle sideslip angle estimation at low speeds and simplified modeling of surrounding vehicle motion states |
| Dynamic single-track | v_x, v_y, r | 1) Considering the longitudinal, lateral and yaw motion; 2) Capable of combining longitudinal dynamics and tire models; 3) Considering longitudinal load transfer | Not considering changes in tire normal force due to lateral load transfer | Suitable for estimating vehicle speed, sideslip angle, tire-road friction, and tire-road forces based on the dynamics of different axles |
| Dynamic double-track | v_x, v_y, r | 1) Capable of considering both longitudinal and lateral load transfer; 2) Capable of describing the vehicle body attitude on uneven roads | High computational burden | Accurately estimate vehicle states by considering 3-DoF tire forces of each tire, especially for 4WD/4WS platforms |

¹ (X, Y) is the coordinates of the vehicle in the ground coordinate system; v_x , and v_y are the longitudinal and lateral velocities, respectively; $\delta\theta$ is the heading angle; r is the yaw rate.

TABLE IV
SUMMARY OF COMMON TIRE MODELS FOR STATE ESTIMATION METHODS OF VEHICLE-ROAD-PEDESTRIAN

| Tire models | Tire dynamics | T.C. | M.A. | C.S. | Scenarios |
|-------------|-----------------|------|------|------|---|
| Linear | | + | J< | 1 | 1) Available in the linear region of tire characteristics; 2) Effectively being used when slip ratio or tire slip angle is small |
| Burckhardt | | 3 | ++ | J< | 1) Available in the linear region and weak nonlinear region of tire characteristics; 2) Model parameters vary significantly under different road surface conditions |
| Dugoff | | | ++ | J. | 1) Available in the linear region and weak nonlinear region of tire characteristics; 2) Not applicable for describing maximum tire force in the strong nonlinear region of tire characteristics |
| Brush | F_x, F_y, M_z | 1 | +++ | J. | Available in most scenarios except the saturated region of tire characteristics |
| MF | F_x, F_y, M_z | 9 | ++++ | J. | Applicable for estimation methods that require high model accuracy |

¹ T.C.: tuning complexity that is denoted by the number of model parameters to be fitted for pure slip (not considering the effect of the vehicle speed on tire dynamics); M.A.: model accuracy; C.S.: combined slip; F_x, F_y, M_z represent the tire longitudinal force, lateral force, and self-aligning torque, respectively; "+" : low; "++": moderate-low; "+++" : moderate-high; "++++": high.

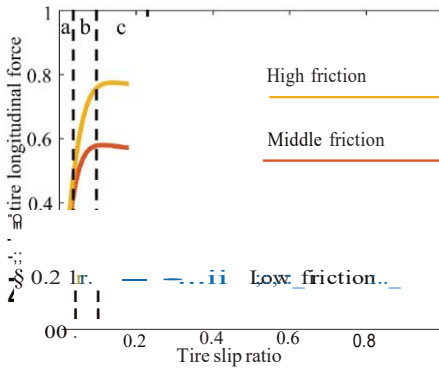


Fig. 6. Illustration of the regions of tire characteristics. "a, b, c" indicate linear region, nonlinear region, and saturated region, respectively (middle friction).

theoretical models, and semi-empirical models. When designing an estimation algorithm, it is crucial to select an appropriate tire model considering the applicable working conditions and tuning complexity. The illustration of the regions of tire characteristics is shown in Fig. 6.

The linear tire model is the simplest theoretical tire model. When the longitudinal slip ratio or tire slip angle is within a certain small range, it can be assumed that the tire force has a linear relationship with the tire longitudinal slip ratio or the tire slip angle. The Burckhardt model, which is an

empirical tire model, can be used to describe both longitudinal and lateral friction characteristics of tires. However, the model generalization is poor due to significant changes in model fitting parameters under different road adhesion conditions. The Dugoff model has a simple structure and can use a few parameters to describe the longitudinal slip and lateral slip characteristics of the tire. In addition, the Brush tire model is also theoretical and is mostly used to describe the lateral friction characteristics of tires [14]. The representative semi-empirical tire model is the Magic Formula (MF). It fits the tire experimental data in the form of a trigonometric function. However, the parameter tuning complexity of the MF tire model is high.

In vehicle modeling, considering the complexity of the models, the most commonly used one is the dynamic single-track model, which satisfies the requirements of most scenarios. To further improve model accuracy in high-speed cornering, the dynamic double-track model is more suitable. As for tire models, the Brush tire model is commonly used for lateral conditions. Additionally, the MF model is more applicable in scenarios that require more precise tire forces.

III. EGO-VEHICLE SIDESLIP ANGLE ESTIMATION

As an indicator for evaluating vehicle stability, the vehicle sideslip angle, which is defined as the angle between the

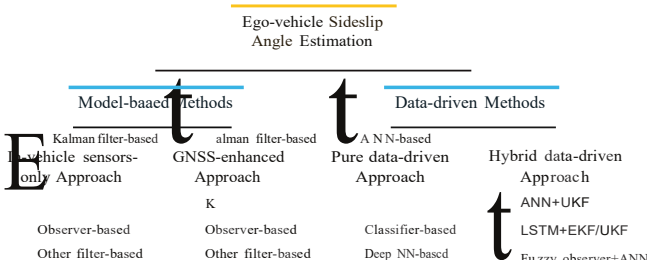


Fig. 7. Classification of ego-vehicle sideslip angle estimation methods. In-vehicle sensors: steering wheel angle sensor, wheel speed sensor, inertial measurement unit, etc. GNSS: global navigation satellite system.

velocity vector and the longitudinal axis of the vehicle coordinate system, cannot be directly acquired by in-vehicle sensors of mass-produced vehicles. The vehicle sideslip angle can only be measured directly by expensive equipments, such as Kistler S-Motion based on the optical flow over ground or high-precision dual-antenna global navigation satellite system (GNSS). Furthermore, compared with the in-vehicle sensors, the measuring rate of the GNSS measurement is lower, and it cannot meet the needs of vehicle motion control under extreme driving conditions. Therefore, real-time and accurate estimation of the vehicle sideslip angle is still a hot research topic [13]. Based on the definition, the vehicle sideslip angle can be obtained by calculating the arctan of the lateral velocity divided by the longitudinal velocity. Generally, the longitudinal velocity of the vehicle can be calculated from the wheel speed of the non-driving wheel. The lateral velocity of the vehicle can be derived by integrating the lateral acceleration output by the IMU. However, the drift and fixed bias error of the gyroscope in the IMU can lead to serious integration errors. In light of this, we mainly focus on the state estimation related to the vehicle sideslip angle and vehicle lateral velocity. Recently, the mainstream methods for the estimation of vehicle sideslip angle can be divided into model-based methods and data-driven methods. The detailed classification of the ego-vehicle sideslip angle estimation methods is presented in Fig. 7.

A. Model-Based Methods for Sideslip Angle Estimation

Generally, low-cost in-vehicle sensors related to vehicle active safety systems mainly include the steering wheel angle sensor, wheel speed sensor, and IMU. Based on the sensor configuration of the existing methods, the model-based methods can be further classified into in-vehicle sensors-only approaches and GNSS-enhanced approaches.

1) In-Vehicle Sensors-Only Approach: Since in-vehicle sensors-only methods have the advantages of low cost, simple deployment, and strong interpretability, in-vehicle sensors-only methods occupy a dominant position in existing vehicle sideslip angle estimation methods, especially the Kalman filter-based methods. The summary of the in-vehicle sensors-only methods is shown in TABLE V. The illustration of Kalman filter (KF)-based methods is shown in Fig. 8.

The KF is a recursive state estimation method that can update the optimal state estimation through the system model and the measured value in a noisy environment. However,

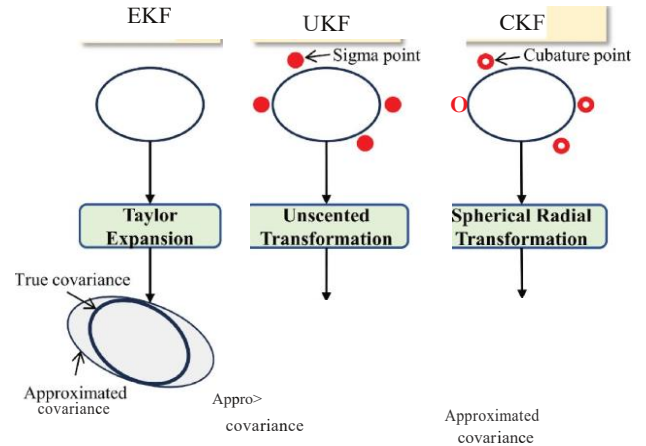


Fig. 8. Illustration of EKF, UKF, and CKF.

in highly dynamic and nonlinear operating conditions, the performance of the methods based on standard KF may degrade. Therefore, many researchers proposed several variations of KF to improve its applicability in nonlinear operating conditions. Considering that the measurement noise is time-varying, the adaptive KF was proposed by online updating the noise covariance [22], [23].

In order to further address the limitations of the traditional KF-based methods, the Extended Kalman Filter (EKF) attracted wide attention. The EKF is an extension of the KF that linearizes nonlinear functions by approximating them using the Taylor series expansion. This enables the computation of the state estimation and variance of the system through the inclusion of first-order terms. Based on the assumption of small tire slip angle under small lateral tire force excitation, some scholars adopted the EKF based on the single-track vehicle model and linear tire model to estimate the sideslip angle [24], [25]. In order to further improve the performance of the standard EKF, complex nonlinear tire models and vehicle models were employed to design EKF-based vehicle sideslip angle estimators, such as the Magic Formula, the dynamic double-track model [26], and multibody vehicle dynamics model [28]. Considering the sensor data loss, Wang et al. [26] proposed a fault-tolerant EKF based on the statistical characteristics of the packet loss. A similar study was also reported in [27] and [29]. Since standard EKF and KF similarly assume that the noise satisfies the Gaussian assumption, traditional EKF performs poorly in time-varying noise environments. In [30], the maximum correntropy criterion was introduced into EKF to improve the estimator performance in non-Gaussian noise situations.

When the tire forces are in the nonlinear region under certain extreme driving conditions, using a first-order linearized EKF may lead to some issues, such as the possibility of estimation divergence when faced with large initial errors and the susceptibility to significant errors caused by linearization. Compared to EKF, the unscented Kalman filter (UKF) utilizes unscented transformations to directly perform nonlinear filtering, thus avoiding local linearization and improving the estimation accuracy of the vehicle sideslip angle under nonlinear conditions. To enhance the performance of the estimators

TABLE V
SUMMARY OF MODEL-BASED EGO-VEHICLE SIDESLIP ANGLE ESTIMATION METHODS USING Low-COST IN-VEHICLE SENSORS ONLY

| Type | Vehicle system model | Methodology | T.C. | O.A. | S.A. | Experiments | Metrics | Year | Ref. |
|----------------|-------------------------------|------------------------|------|------|------|-------------|-------------|------|------|
| KF-based | 2-DoF single-track+Linear | Adaptive KF | + |)< |)< | SIM/ONR | AE/RMSFJCVT | 2019 | [22] |
| | 7-DoF double-track+MF | Dual difference KF | + | Vi" |)< | SIM | AE | 2023 | [23] |
| EKF-based | 2-DoF single-track+Linear | Adaptive EKF | + |)< | Vi" | SIM/ONR | RMSE | 2019 | [24] |
| | 3-DoF single-track+Linear | Fusion-based EKF | + |)< |)< | SIM/ONR | RMSE | 2020 | [25] |
| | 7-DoF double-track+MF | Fault-tolerant EKF | + |)< |)< | SIM/ONR | RMSE | 2021 | [26] |
| | 7-DoF double-track+MF | Fault-tolerant EKF | + |)< | Vi" | SIM | RMSE | 2022 | [27] |
| | Multibody model+MF | Adaptive EKF | + |)< |)< | SIM/ONR | AE | 2023 | [28] |
| | 3-DoF single-track+Linear | Fault-tolerant EKF | + |)< |)< | SIM/ONR | RMSE | 2023 | [29] |
| | 3-DoF single-track+Linear | MCC-based EKF | + |)< |)< | SIM | RMSE | 2023 | [30] |
| UKF-based | 7-DoF double-track+MF | IMM-based STUKF | +++ |)< |)< | SIM/ONR | MAFJCVT | 2020 | [31] |
| | 7-DoF double-track+MF | Adaptive UKF | +++ |)< |)< | SIM/ONR | RMSE | 2022 | [32] |
| | 7-DoF double-track+HRSI | Adaptive UKF | +++ |)< |)< | SIM | RMSFJCPT | 2022 | [33] |
| CKF-based | 2-DoF single-track+Linear | Adaptive CKF | ++ |)< |)< | SIM/ONR | RMSFJMAE | 2022 | [34] |
| | 7-DoF double-track+MF | Adaptive SRCKF | ++ |)< |)< | SIM/ONR | RMSFJMAE | 2022 | [35] |
| | 3-axle single-track+Linear/MF | Adaptive CKF | ++ |)< |)< | SIM/HIL | RMSE | 2023 | [36] |
| | 7-DoF double-track+MF | ST-SRCKF | ++ | Vi" |)< | SIM/HIL | MAE/RMSE | 2023 | [37] |
| Observer-based | 7-DoF double-track+MF | MHE | +++ | Vi" |)< | SIM | AE/RMSFJCVT | 2019 | [38] |
| | 3-DoF single-track+Linear | LPV UI observer | +++ |)< | Vi" | HIL | MAE/RMSE | 2019 | [39] |
| | 2-DoF single-track+Linear | Interconnect observers | +++ |)< | Vi" | HIL | AE | 2021 | [40] |
| | 2-DoF single-track+MF | Fuzzy UI observer | +++ |)< | Vi" | HIL | MAE/RMSE | 2021 | [41] |
| | 2-DoF single-track+Linear | ET T-S observer | +++ |)< | Vi" | SIM | AE | 2022 | [42] |
| | 2-DoF single-track+Dugoff | Switch T-S observer | +++ |)< | Vi" | ONR | MFJRMSE | 2022 | [43] |
| | 2-DoF single-track+Linear | ET Hoo observer | +++ |)< | Vi" | SIM/ONR | RMSE | 2023 | [44] |

¹ Common low-cost in-vehicle sensors: steering wheel angle sensor, wheel speed sensor, and IMU, etc.

² T.C.: tuning complexity; O.A.: observability analysis; S.A.: stability analysis; MCC: maximum correntropy criterion; ST: strong tracking; ET: event-triggered; MHE: moving horizon estimator; LPV: linear parameter-varying; UI: unknown input; SIM: simulation; HIL: hardware-in-loop; ONR: on-road test; RMSE: root mean squared error; AE: absolute error; CPT: computation time; CVT: convergence time; MAE: mean absolute error; "+" low; "++": moderate; "+++": high.

in a time-varying system structure, the strong tracking theory was introduced into the UKF [31]. Other adaptive UKF methods were also intensively reported in recent years [32], [33].

The cubature Kalman filter (CKF) is founded on the third-order spherical-radial volume criterion, whereas the UKF algorithm is not. It utilizes a set of volume points to approximate the state mean and covariance of the nonlinear system with additive Gaussian white noise. CKF reduces the computational burden and ensures the positive definiteness of the prediction matrix. In [34], [35], and [36], the adaptive CKF estimator was proposed to dynamically update the process noise parameters. Considering the influence of road inclinations, Liu et al. [37] introduced a strong tracking theory into the CKF. It is worth noting that the tuning complexity of CKF-based methods is smaller than that of UKF-based methods [45]. In addition to the nonlinear KP-based methods, observer-based methods were also adopted in the estimation of vehicle sideslip angle [38], [39], [40], [41], [42], [43], [44].

2) *GNSS-Enhanced Approach*: With the continuous development of intelligent transportation systems, the application of more sensors has provided new opportunities for research in vehicle state estimation, such as cameras, LiDAR, and GNSS [58]. The measurements from GNSS are robust to the high dynamic changes of the tire-road and vehicle dynamics models. It is worth discussing recent estimation methods based on the fusion of GNSS and other onboard sensors. Generally, GNSS can directly provide accurate vehicle position and speed information when GNSS signals are available. However, the

TABLE VI
SUMMARY OF MODEL-BASED EGO-VEHICLE SIDESLIP ANGLE ESTIMATION METHODS WITH GNSS AUGMENTATION

| Method | V.D. | O.A. | S.A. | Metric | Year |
|--------------|------|------|------|----------|-----------|
| Adapti |)< |)< |)< | MAE/I | 2020 |
| SRCK |)< |)< |)< | AE | 2021 |
| Adapti |)< | Vi" |)< | MAE/I | 2021 |
| | | | | | 2021 |
| ET-KF |)< |)< | Vi" | MAE/I | 2022 |
| Invari |)< |)< |)< | MAE | 2023 |
| Augm | Vi" | Vi" |)< | MAE/I | 2021 |
| Sliding | Vi" |)< | Vi" | RMSE | 2021 |
| IMM-I | Vi" | Vi" |)< | MAE/I | 2022 |
| MHE | Vi" |)< |)< | AE | 2022 |
| Adapti | Vi" |)< |)< | MAE/I | 2022 |
| Consensus KF | Vi" | Vi" | Vi" | MAE/RMSE | 2023 [57] |

¹ VD.: considering vehicle dynamics; S.A.: stability analysis; O.A.: observability analysis; Ref.: references

² ET: event-triggered; MHE: moving horizon estimator; RMSE: root mean squared error; AE: absolute error; MAE: mean absolute error.

update frequency of GNSS is relatively low, and its signals are easily obstructed by buildings. To compensate for this deficiency, GNSS signals are introduced into kinematics-based estimation algorithms. Typically, the drift and stochastic errors of the IMU are modeled in the estimation algorithm based on the fusion of GNSS and IMU signals. Since the value of the heading angle error is comparable to the vehicle sideslip

estimation error, Xia et al. [48] established the observability index for the estimator and designed a hybrid feedback strategy to correct the heading angle error of the inertial navigation system. A simplified vehicle roll model was constructed to alleviate the impact of vehicle roll motion on the lateral acceleration measured by the IMU. Then an event-triggered KP was designed to eliminate cumulative errors in vehicle sideslip angle estimation [50]. Other similar kinematics-based studies with the fusion of GNSS and IMU information in recent years can also be found in [46], [47], [49], and [51].

The knowledge of the tire-road dynamics is not required in kinematics-based estimation methods. However, the integration errors caused by biases and misalignment in the measurements of IMU can have a negative impact on kinematics-based estimation methods. Therefore, integrating vehicle kinematics and dynamics models to estimate the vehicle sideslip angle with the assistance of GNSS is currently one of the research hotspots. Considering the model uncertainty under nonlinear conditions, a longitudinal velocity error compensation model was established based on a low-cost GNSS. Then a robust sliding mode observer was designed to estimate the lateral velocity of the vehicle [53]. Similar studies that benefit from the low-cost GNSS can also be found in [54] and [55]. Considering the low estimation accuracy of kinematics-based methods with the small lateral excitation, the heading angle error was introduced into the vehicle velocity estimation to enhance its observability [52], [56], [57]. The summary of GNSS-enhanced methods is presented in TABLE VI.

B. Data-Driven Methods for Sideslip Angle Estimation

In recent years, neural network-based artificial intelligence technologies have developed rapidly. Inspired by this, the data-driven multi-source sensor method is used to estimate the ego-vehicle sideslip angle. Data-driven methods can be pure or hybrid, depending on whether model-based and data-driven methods are combined.

1) *Pure Data-Driven Approach*: As shown in Fig. 9, the pure data-driven approach primarily employs an end-to-end data fitting process to learn the nonlinear mapping relationship between input and output. Most methods rely on vehicle dynamic information collected by in-vehicle sensors to train artificial neural network (ANN)-based methods [59], [60], time-delay neural network (TDNN)-based methods [61], RNN-based methods [62].

2) *Hybrid Data-Driven Approach*: Since pure data-driven methods rely more on high-quality training data, model-based methods are not affected by differences in individual vehicle dynamic characteristics. However, under extreme driving conditions with strong time-varying nonlinearity, the estimation performance of model-based methods may decrease due to the difficulty in establishing accurate physics models. Considering the powerful nonlinear fitting advantages of data-driven methods, the combination of data-driven methods and model-based methods received more and more attention. Based on the vehicle kinematics model, some researchers combined ANN and KP-based methods to estimate vehicle sideslip angle [63], [64]. Similar studies combining observer-based

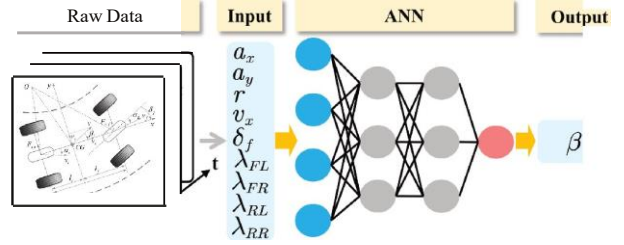


Fig. 9. Illustration of ANN-based approach for vehicle sideslip angle estimation [59]. a_x and a_y are longitudinal and lateral acceleration, respectively; δ_f is front wheel steering angle; $\lambda_{..j}$ denotes the slip ratio of each wheel; β indicates vehicle sideslip angle.

methods with ANNs were also conducted in [65] and [66]. Moreover, a fusion method based on long short-term memory neural network (LSTM) and KP-based methods was proposed for vehicle sideslip angle estimation [67], [68]. For vehicle lateral velocity estimation, similar studies were also reported in [69], [70], and [71]. In addition, the estimation methods that embed physical information into neural networks were also proposed to enhance interpretability and generalization capabilities [72], [73]. Considering that accurate vehicle modeling is time-consuming, a KP-based method based on a digital twin vehicle model was proposed and the Bayesian optimization was utilized to tune the parameters of the estimator [74].

C. Recent Trends of Sideslip Angle Estimation in 4WD/4WS

With the advancement of electric vehicle technology, the layout of four-wheel drive (4WD) electric vehicles equipped with in-wheel motors has emerged as the new paradigm in modern electric vehicle development. The wheel torque of 4WD electric vehicles equipped with in-wheel motors is measurable. It can be precisely controlled, thereby achieving superior chassis control performance compared to traditional front-wheel drive electric vehicles. However, since each wheel can serve as a driving wheel, it is challenging to estimate the longitudinal vehicle speed using the wheel speed of non-driven wheels, as is done in conventional vehicles, particularly when the slip ratio of the driven wheels is high. Therefore, the above characteristics also bring new opportunities and challenges to vehicle state estimation based on 4WD electric vehicle platforms. In recent years, the following estimation techniques of vehicle sideslip angle have been widely studied on 4WD electric vehicle platforms, such as adaptive KP [23], UKP [75], [76], CKP [35], particle filter [77], unknown input observer [78], and TDNN [61]. In addition, for the four-wheel steering (4WS) platform, unlike common vehicles with only front-wheel steering, it is necessary to consider rear-wheel steering in vehicle modeling. The following methods were proposed for vehicle sideslip angle estimation of this platform, such as UKP [79] and particle filter [80].

Given the diverse benefits of vehicle kinematics and dynamics models in various scenarios, achieving accurate estimation through model-based methods usually needs precise modeling. Compared with model-based methods, data-driven methods, which do not rely on precise physical models, are sensitive to data quality and may lack generalization capabilities across

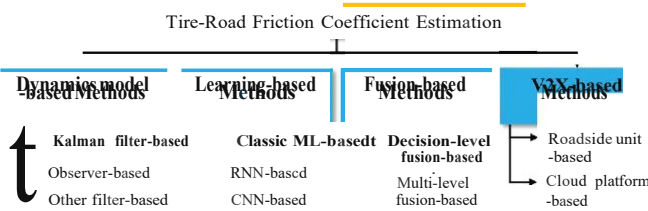


Fig. 10. Classification of TRFC estimation methods. ML: machine learning; RNN: recurrent neural network; CNN: convolutional neural network.

different mass-produced vehicles. Thus, the integration of vehicle kinematics and dynamics with multisensor information emerges as a promising direction for future research.

IV. ROAD SURFACE STATE ESTIMATION

Since the driving performance of the vehicle ultimately depends on the interaction between the tire and the road surface, the change in road surface states caused by weather and other factors can directly affect the vehicle's stability. Among road surface states, the TRFC and road unevenness have a significant impact on vehicle driving safety and occupant comfort. Accurate pre-identification and timely acquisition of these road surface states are crucial for both AVs and CAVs.

A. Tire-Road Friction Coefficient Estimation

The performance of vehicle active safety systems, which aim to stabilize the vehicle through tire force control, heavily relies on ensuring that the computed tire force command remains within the friction limit. Thus, the knowledge of TRFC is crucial to achieve accurate vehicle motion control. Moreover, TRFC is also an important input for intelligent vehicle decision-making and planning layers [81]. However, in-vehicle sensors in mass-produced vehicles cannot directly measure TRFC, and even advanced perception sensors (i.e., camera, radar, and LiDAR) of ITS still do not support direct acquisition of TRFC. Therefore, TRFC estimation has been extensively studied in recent years. As shown in Fig. 10, the recent existing estimation methods can be roughly divided into dynamics-based methods, learning-based methods, fusion-based methods, and V2X-based methods.

1) Dynamics Model-Based Methods for TRFC Estimation:

The dynamics model-based methods mainly use the vehicle dynamic response measured by in-vehicle sensors to estimate TRFC. These methods are mainly designed based on the principle that the slope of the tire force characteristic curve is different under various TRFCs in the same slip ratio or tire slip angle. Generally, the methods based on vehicle longitudinal dynamics often require a vehicle to perform large acceleration and deceleration operations to obtain sufficient longitudinal tire force excitation [97]. On the other hand, the estimation methods based on lateral dynamics require a relatively small amount of lateral tire force excitation generated by the self-aligning torque. In addition, lateral stability control is more important than longitudinal stability control to prevent dangerous conditions such as tail-throwing. For this reason, many scholars designed nonlinear observers to estimate TRFC under vehicle steering maneuvers by utilizing Brush tire model [82],

TMSimple tire model [83], HSRI tire model [84]. A similar study for lateral excitation was also reported in [85].

In real driving conditions, it is common to perform acceleration and steering maneuvers simultaneously, which results in tire-road dynamics often being involved in dynamic coupling. The methods based on the pure lateral tire dynamics may lead to unreasonable estimation results. Therefore, some scholars proposed estimation methods for coupling excitation. To overcome the potential drawbacks of the EKF, an adaptive UKF algorithm for TRFC estimation received widespread attention, such as in [86], [87], and [88]. Considering the situation of sensor signal loss, a fault-tolerant UKF was designed in [89]. Recently, the more advanced CKF was adopted by researchers for TRFC estimation. An adaptive square root CKF was proposed for TRFC estimation, where the process noise can be dynamically updated based on the lateral acceleration [90]. Similar studies were also conducted in [91], [92], and [93]. The particle filter (PF)-based methods, which utilized Monte Carlo techniques to approximate the posterior distribution of the state, were also employed for TRFC estimation [94], [95]. Considering that the convergence speed of filter-based estimation methods is limited by specific excitations, the TRFC can be rapidly estimated by numerically inverting the tire model that describes the relationship between tire forces and grip margin [98], [99]. For instance, the model inversion-based methods using the Brush tire model have been further studied over the past few years [96], [100], [101]. Algebraic computation is used to avoid the convergence requirements of filter-based estimators and the excitation level requirements of tire-road excitations. It is worth noting that this method can only be used with simple tire models, such as the Brush tire model, and the estimation accuracy is susceptible to tire modeling accuracy. In order to facilitate the comparison of various methods, the recent common estimation methods based on vehicle dynamics are shown in TABLE VII.

2) *Learning-Based Methods for TRFC Estimation*: With the development of artificial intelligence techniques, learning-based methods, represented by neural networks, were applied to TRFC estimation. Similar to the pure data-driven approach discussed in Section III, some researchers also explored the use of vehicle dynamic information collected through in-vehicle sensors to train neural networks for establishing nonlinear mapping estimations of TRFC, such as TDNN [102], gated recurrent units (GRU) [103], LSTM [104], ANN [108], and fuzzy neural networks [109]. In addition, other classic machine learning-based methods using in-vehicle sensors were also reported, including online Bayesian inference [105], adaptive Monte-Carlo Markov chain (MCMC) [106], and random forest learning [107]. However, the performance of the above methods could be influenced by the accuracy of measured TRFC in the training data.

With the development of vehicle intelligence, an increasing number of intelligent vehicles are equipped with environmental perception sensors such as cameras and LiDAR. In recent years, there has been a significant improvement in the multisensor information processing capabilities of intelligent vehicles due to the enhanced computational power of on-board controllers. Cameras are widely used perception sensors

TABLE VII
SUMMARY OF DYNAMICS MODEL-BASED TRFC ESTIMATION METHODS

| Type | Vehicle system model | Methodology | T.C. | S.A. | M.E. | Experiments | Metrics | Year | Ref. |
|-----------------|-------------------------------|--------------------|------|------|---------|-------------|----------|------|------|
| Observer-based | 2-DoF single-track+Brush | Nonlinear observer | +++ |)< | ONR | AE/CVT | 2019 | [82] | |
| | 2-DoF single-track+TMSimple | Nonlinear observer | +++ |)< | SIM/ONR | AE | 2019 | [83] | |
| | 3-DoF single-track+HSRI | MHE | +++ |)< |)< | SIM | AE | 2020 | [84] |
| UKF-based | 2-DoF single-track+Brush | Cascade UKF | +++ |)< |)< | SIM | AE/CVT | 2020 | [85] |
| | 7-DoF double-track+MF | IMM-based STUKF | +++ |)< |)< | SIM/ONR | MAE/CVT | 2020 | [31] |
| | Multibody model+TMeasy | Adaptive UKF | +++ |)< |)< | SIM | RMSFJCVT | 2021 | [86] |
| | 3-DoF single-track+Brush | Adaptive UKF | +++ |)< |)< | SIM/ONR | MFJCVT | 2022 | [87] |
| | 3-DoF single-track+Brush | IMM-based STUKF | +++ |)< |)< | ONR | RMSE | 2022 | [88] |
| CKF-based | 7-DoF double-track+Brush | ET-FTUKF | +++ |)< |)< | SIM/HIL | RMSE | 2023 | [89] |
| | 7-DoF double-track+MF | Adaptive SRCKF | ++ |)< |)< | SIM/ONR | AE | 2022 | [90] |
| | 7-DoF double-track+Dugoff | STCKF | ++ |)< |)< | SIM/ONR | RMSE | 2023 | [91] |
| PF-based | 7-DoF double-track+Dugoff | ST-SRCKF | ++ |)< |)< | SIM/ONR | RMSFJCVT | 2023 | [92] |
| | 7-DoF double-track+Dugoff | SRCKF | ++ |)< |)< | SIM/ONR | AE/CVT | 2023 | [93] |
| | 7-DoF double-track+Burckhardt | Particle filter | +++ |)< |)< | HIL | RMSFJCVT | 2022 | [94] |
| Inversion-based | Modified Brush | Model inversion | ++ |)< |)< | ONR | AE/CVT | 2020 | [96] |

¹ T.C.: tuning complexity; S.A.: stability analysis; M.E.: considering modeling errors.

² ET: event-triggered; MHE: moving horizon estimator; SIM: simulation; HIL: hardware-in-loop; ONR: on-road test; RMSE: root mean squared error; AE: absolute error; MAE: mean absolute error; CPT: computation time; CVT: convergence time; "++": moderate; "+++": high.

TABLE VIII
SUMMARY OF LEARNING-BASED TRFC ESTIMATION METHODS

| Type | Methodology | G.C. | Night | C.B. | Year | Ref. |
|--------------|--------------------|------|-------|------|------|-----------------|
| NS-based | TDNN | + | | ++ | 2019 | [102] |
| | GRU | + | | ++ | 2020 | [103] |
| | LSTM | + | | ++ | 2021 | [104] |
| | Bayesian inference | + | | ++ | 2021 | [105] |
| | Adaptive MCMC | + | | ++ | 2022 | [106] |
| | Random forest | + | | + | 2022 | [107] |
| | ANN | + | | ++ | 2023 | [108], 2023 |
| Camera-based | KE-VGGNet | +++ |)< | +++ | 2020 | [110] |
| | ResNet | ++ |)< | ++ | 2020 | [111] |
| | DS-ShuffleNet | +++ |)< | ++ | 2021 | [112], 2022 |
| | | | | | 2023 | [113], [114] |
| | MDAN | ++ |)< | +++ | 2022 | [115] |
| LiDAR-based | MobileNet-v2 | ++ |)< | ++ | 2022 | [116] |
| | VGGNet | +++ | | +++ | 2022 | [117] |
| | SVM | +++ | | +++ | 2023 | [118] |

¹ G.C.: generalization capability; C.B.: computational burden; NS: in-vehicle sensors; KE: knowledge-embedded; AFNN: asymmetric fuzzy neural network; DS: Dempster-Shafer evidence theory; MDAN: multi-task distillation attention network; "+": low; "++": moderate; "+++": high.

in intelligent vehicles. For this reason, many researchers conducted studies on TRFC estimation using cameras, such as prior knowledge-based VGGNet [110], modified ResNet [111], ShuffleNet based on improved Dempster-Shafer evidence theory [112], [113], [114], multi-task distillation attention network [115], and MobileNet-v2 [116]. Due to the inability of camera-based methods to operate in nighttime environments, some researchers applied support vector machine (SVM) and CNN models based on the principle that the laser reflection intensity varies with different road textures to establish a mapping relationship between reflection

intensity and TRFC, thereby achieving TRFC estimation [117], [118]. In order to facilitate the comparison of various methods, the summary of the above recent learning-based estimation methods is shown in TABLE VIII.

3) Fusion Algorithm-Based Methods for TRFC Estimation: Dynamics model-based methods and learning-based methods have their advantages in different working conditions. Data acquired by traditional in-vehicle sensors is often accompanied by signal noise and external disturbances, and visual perception sensor data is susceptible to interference from the external environment. Therefore, the TRFC estimation methods based

on a single information source have certain limitations. Based on the multi-source information fusion theory [81], some scholars combined the strengths of these two approaches to designing TRFC estimation methods based on the fusion of vehicle dynamics and machine vision. Multi-source information fusion can generally be divided into three levels of fusion: data-level fusion, feature-level fusion, and decision-level fusion. For the decision-level fusion, Leng et al. [119] first proposed a dynamic and visual fusion estimator. Building upon this, Tian et al. [120] further considered model uncertainty and introduced the improved Dempster-Shafer evidence theory to enhance estimation accuracy.

Since the multi-level fusion method has better estimation accuracy and robustness, multi-level fusion estimation methods were initially explored in recent years [121], [122], [123]. In order to avoid unreasonable fusion estimation results, a fusion estimation framework based on multi-source information assessment was proposed in [81].

4) V2X-Based Methods for TRFC Estimation: In recent years, the development of V2X technology enabled the sharing of TRFC estimation results in the time and spatial dimensions of intelligent transportation systems. This allows for the advance sharing of predicted TRFC with the moving vehicles and timely notification to traffic management authorities to

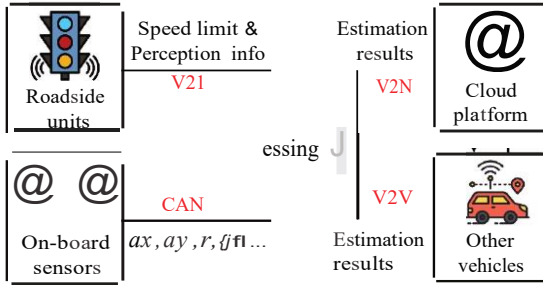


Fig. 11. Illustration V2X-based TRFC estimation methods [124], [125], where ax and ay are longitudinal and lateral acceleration of the vehicle body, respectively; r denotes the yaw rate of the vehicle body; $8f$ denotes front wheel steering angle.

restrict traffic flow density on corresponding slippery road sections, thereby further enhancing road traffic safety [126]. Based on the roadside unit, a machine learning-based regression classifier was proposed in [125] to estimate the current TRFC range of the road and send recommended speed limits to the connected vehicles. Based on a vehicle-road network cloud system, Li et al. [127] proposed a deep learning model combining CNN and LSTM for TRFC estimation. A similar study was also reported in [128]. Considering that V2X technology enables long-range perception, the road friction map based on intelligent transportation systems received more and more attention from researchers [124], [129], [130]. The road friction map at intersections can issue warnings about slippery road conditions to other connected vehicles, which can better ensure the operational efficiency and safety of ITS. The illustration of V2X-based TRFC estimation methods is presented in Fig. 11.

5) Tire Normal Force Estimation: The variation in tire normal force directly impacts tire dynamics and consequently affects the peak tire friction force. According to the definition of TRFC, tire normal force also plays a significant role in the estimation of TRFC. Typically, considering the load transfer effect during vehicle operation, the tire vertical load on the left front wheel on a horizontal road can be expressed as follows:

$$F_{zfl} = \frac{mgl_r}{2l} - \frac{ma_x h}{2l} - \frac{may_l r_h}{bf} \quad (1)$$

where m denotes the vehicle mass, l is the wheelbase, Z_r is the distance between the rear axle and the vehicle center of gravity, bf denotes the track width of the front wheels, and h represents the vehicle center of gravity height.

Although the tire normal force estimation can be performed using (1), the TRFC estimation can benefit from a more accurate estimation of tire normal forces. In real driving conditions, the vehicle mass and the vehicle center of gravity height may deviate from their nominal values, leading to errors in the estimation of tire normal force. Generally, the vehicle mass can be estimated based on longitudinal dynamics using the recursive least squares algorithm, and various other estimation methods have been extensively studied in recent years [131]. Therefore, in what follows, we focus on the estimation of the vehicle center of gravity height and the online estimation of tire normal force.

Based on dynamic models, some researchers have extensively studied the estimation of the vehicle center of gravity height, employing methods such as observer-based approaches [132] and KF-based methods [87], [133]. These dynamics-based methods typically require specific excitations to satisfy the conditions of system observability. However, this can negatively impact passenger comfort and vehicle stability. Therefore, Xu et al. [134] proposed a method that does not require dynamic excitation. This approach utilizes roadside sensors to capture images of the vehicle, the vehicle's basic dimensional parameters, and vehicle mass. An improved YOLO algorithm is then used to identify the vehicle type, followed by a regressor to predict the vehicle center of gravity height.

Moreover, some scholars considered the suspension dynamics to improve the estimation accuracy of the tire normal force. Based on the vertical acceleration signal of the IMU, the effect of vehicle roll dynamics was integrated into the basic load transfer model to obtain more accurate estimation results [71]. Similar studies were also proposed based on the more complex suspension model [135], [136]. In addition, considering the influence of road inclinations, the tire normal fore estimation was further explored [37], [137].

6) Recent Trends of TRFC Estimation in 4WD/4WS: Since the accurate wheel torque information and wheel speed of 4WD electric vehicles are known, tire forces and TRFC can be estimated based on the single-wheel dynamics and tire models. Therefore, in recent years, similar to ego-vehicle sideslip angle estimation, the TRFC and tire-road force estimation research has also benefited from this feature of 4WD electric vehicles, including dynamics model-based methods [76], [80], [84], [90], [91], [92], [93], [94], [136], NN-based methods [109], and fusion-based methods [81], [119], [120], [121].

B. Road Unevenness Pre-Identification

As one of the key road surface states, uneven roads will significantly affect vehicle vertical motion states and occupant comfort. Road unevenness can be categorized into different levels based on the profile power spectral density. Among them, some responses with short wavelengths caused by short road cracks can be filtered by tires. However, serious road defects (e.g., road bumps, potholes, obstacles, etc.) can transiently impact vehicles and easily affect vehicle driving safety. Road unevenness estimation methods can be mainly divided into dynamic response-based and preview-based methods. The performance of dynamic response-based methods is limited by the excitation from the road surface. As a result, it cannot preview the unevenness of the road ahead [138]. Therefore, this subsection will briefly review the recent preview-based road unevenness estimation methods for vehicle safety control.

Since model-based preview estimation algorithms [139], [140] may lack robustness to unconsidered road roughness conditions, data-driven algorithms have recently received more attention. Existing data-driven preview-based estimation methods for intelligent vehicles can be mainly divided into image-based methods and point cloud-based methods [141]. Image-based preview estimation methods have been extensively studied in recent years, including object detection-based

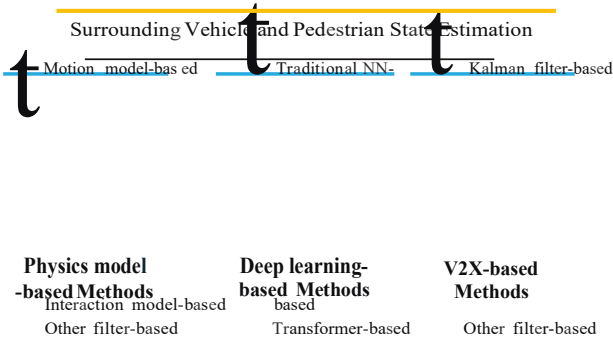


Fig. 12. Classification of surrounding vehicle and pedestrian state estimation methods.

approaches [142], [143], [144] and semantic segmentation-based approaches [145], [146].

However, the performance of onboard cameras is susceptible to lighting conditions, and the captured images can suffer from motion blur due to high vehicle speed. Consequently, point cloud-based data-driven unevenness estimation methods can emerge as promising solutions. Compared to image-based methods, they can better distinguish between road potholes and cracks. For instance, Zhao et al. [147] proposed a hierarchical road surface unevenness perception framework based on PointNet++. This framework segments the point clouds corresponding to irregular road areas and outputs the geometric dimensions of road bumps or potholes from the segmented point clouds, allowing the vehicle control system to make appropriate adjustments.

Compared to the demands of road maintenance, road unevenness estimation for the safety and comfort control of autonomous vehicles focuses on severe road defects and requires higher real-time performance and accuracy. Additionally, algorithms based on multi-frame fused point cloud data impose higher demands on the real-time processing capabilities of the system. There remains considerable potential for the development of methods that fuse visual and point cloud data. Details on other road defect detection methods aimed at road maintenance can be found in [141].

C. Recent Industrial Solutions for Tire-Road State Estimation

Since most of the methods reviewed above rely on various sensors installed on the vehicle, they are more or less limited by the accuracy of the sensor measurements. Therefore, the industry has also been committed to developing products that directly measure tire states in recent years. The current industrial products developed for the market can be mainly divided into smart tires and load sensing bearings [18].

Smart tires are typically embedded with various sensors that monitor the internal and external states of the tire. The tire manufacturer Pirelli Tyre S.p.A. developed a smart tire system called Cyber™ Tire, which can measure the normal force and longitudinal force of the tire, as well as detect hydroplaning. Currently, the McLaren Artura hybrid supercar is equipped with Pirelli's Cyber™ tire technology [148]. In addition, another leading company in the tire industry, the Goodyear Tire and Rubber Company, has collaborated with the Dutch research institute TNO to apply its SightLine™ intelligent tire technologies in ABS [149]. Furthermore, other renowned

Another notable example is the load sensing bearings introduced by the Swedish bearing manufacturer SKF. In addition

Unlike smart tires, which are prone to tire wear, bearings

to the original function of the bearing, the sensing bearings can also measure tire forces through the strain on the bearing. automotive manufacturers and component suppliers are also actively developing intelligent tires, such as Continental AG, Hyundai Motor, etc [150].

have a longer service life. Moreover, the load sensing bearings benefit from their installation position, which allows for more accurate measurements. This sensing bearing was further applied in the estimation of TRFC and vehicle sideslip angle [151], [152]. However, due to cost factors and additional measurement noises, the potential for widespread application of smart tires and load sensing bearings deserves further exploration.

Similar to the characteristics of model-based ego-vehicle sideslip angle estimation methods, dynamics model-based methods are influenced by the accuracy of physical model modeling. Moreover, the performance of the vehicle dynamic model exhibits strong time-varying characteristics under highly nonlinear conditions. Inaccurate modeling can result from factors such as tire wear and actuator wear, and the estimation accuracy is also susceptible to longitudinal and lateral dynamic excitations of the vehicle. Additionally, learning-based methods based on perception sensors are susceptible to environmental factors, such as poor lighting conditions, heavy snow, and thick fog, which can impair the normal functioning of the perception sensors. However, learning-based methods based on perception sensors can achieve estimation without the need for dynamic excitations. On the other hand, V2X-based and fusion-based methods are still in their early stages. Therefore, fusion methods that incorporate V2X technology and other multi-sensor information should receive more attention in the future, and the distribution map of TRFC will become important state information for ITS.

V. SURROUNDING VEHICLE AND PEDESTRIAN STATE ESTIMATION

The mixed traffic mode of traditional human-driven vehicles, connected vehicles, and vulnerable participants is considered to be the most promising mode of future intelligent transportation systems [3]. Thus, accurate information on the motion states of other traffic participants is as important as ego-vehicle system states and road surface states. Since the multi-object tracking provides the current and previous motion state estimates of surrounding traffic participants, it can serve as an important input for the subsequent trajectory prediction module. Therefore, it is a key component of the autonomous driving technology. Multi-object tracking is a hot research topic in the field of computer vision. It involves detecting targets in individual frames and identifying the same object in subsequent frames. Multi-object tracking algorithms typically include object localization, feature extraction, data association, and tracking management [15].

According to the defined scope in Section I, this section highlights object localization module research. In particular, object localization involves tracking an object's location and potential direction or speed over time. Fig. 12 summarizes the motion state estimation methods for surrounding vehicles and pedestrians.

TABLE IX
SUMMARY OF PHYSICS MODEL-BASED SURROUNDING VEHICLE STATE ESTIMATION METHODS

| Model | Methodology | T.C. | S.A. | L.S. | Year | Ref. |
|-----------------|--------------------|------|------|------|------|----------------------|
| CV | Correlation filter | + |)< |)< | 2022 | [153] |
| VKM | Adaptive KF | + |)< |)< | 2023 | [154] |
| CV+CTRA | Nonlinear observer | +++ | .I' | .I' | 2019 | [155] |
| CV | IMM-KF | ++ |)< | .I' | 2019 | [156] |
| VKM | Nonlinear observer | +++ | .I' | .I't | 2020 | [157], 2023 [158] |
| CTRA | Adaptive KF | + |)< | .I't | 2021 | [159] |
| VDM | MHE | +++ |)< | .I't | 2021 | [160] |
| CV | Nonlinear observer | +++ | .I' | .I' | 2022 | [161] |
| NCA+CTRPV | IMM-EKF | ++ |)< | .I' | 2023 | [162] |
| VKM | MHE | +++ |)< | .I' | 2023 | [163] |
| IDM+MOBIL | Particle filter | +++ |)< | .I' | 2019 | [164] |
| IDM+MOBIL | UKF | +++ |)< | .I' | 2019 | [165] |
| Potential force | Particle filter | +++ |)< | .I' | 2020 | [166] |
| Graph model | Interactive KF | +++ |)< | .I' | 2020 | [167], 2022 [168] |

¹T.C.: tuning complexity; S.A.: stability analysis; L.S.: vehicle lateral states; t: including yaw rate or yaw angle.

²VKM: vehicle kinematics model; VDM: vehicle dynamics model; CV: constant velocity model; CTRPV: constant turn rate and constant polar velocity model; CTRA: constant turn rate and constant acceleration model; NCA: nearly constant acceleration model; IMM: interacting multiple model; MHE: moving horizon estimator; IDM: car-following model; MOBIL: lane-changing model; "+": low; "++": moderate; "+++": high.

A. Surrounding Vehicle State Estimation

For the surrounding vehicles, the motion states mainly include vehicle position, longitudinal speed, lateral speed, and yaw rate. In summary, the multi-object tracking task can be decoupled into object detection and data association. Since the detection-free tracking paradigm cannot handle new tracking targets, most existing research adopts the detection-based tracking paradigm [19].

1) *Physics Model-Based Methods for Surrounding Vehicle State Estimation:* Based on whether the interaction between traffic participants is considered, the physics model-based methods can be further categorized into motion model-based approaches and interaction model-based approaches [19].

The motion model-based approach mainly establishes a mathematical model for the observation object to predict the position of the target in future frames. The motion models are mainly divided into linear and nonlinear motion models. In recent years, the estimation methods based on the constant velocity model were extensively studied [153], [156], [161]. The methods based on the constant velocity model assume that the target moves linearly, which is acceptable at very short occlusion periods. Some researchers further explored the methods based on the nonlinear motion models [154].

The lateral motion states of the surrounding vehicle are also crucial to the planning and control system of the host vehicle [169]. A full understanding of the lateral motion behavior of the surrounding vehicle is conducive to further promoting the traffic safety of intelligent transportation systems. In recent years, most researchers tended to conduct lateral modeling first and then design estimation algorithms, such as IMM-based KF [156], UKF [159], and IMM-based EKF [162]. In addition, nonlinear observers were also designed to estimate

lateral motion states of surrounding vehicles [155], [157], [158], [160], [161], [163]. It is worth noting that the yaw rate and yaw angle of the surrounding vehicles can be estimated by the proposed methods in [157], [158], [159], and [160].

Considering that when tracking multiple vehicles, the motion behaviors of multiple vehicles can affect each other, the interaction model-based approach mainly uses modeling to describe the interactive relationship of the tracking target. To solve the problems caused by conventional multi-vehicle tracking algorithms assuming that vehicles move independently of each other, more and more researchers introduced the interaction models between traffic participants into the estimation methods, such as IDM and MOBIL model [164], [165], potential force model [166], and interaction graph model [167], [168]. Although the interaction model improves the estimation performance of the algorithm in the case of large occlusions, the time-consuming of the algorithm requires further attention. The detail of the above methods is presented in TABLE IX.

2) *Traditional NN-Based Methods for Surrounding Vehicle State Estimation:* With the development of artificial intelligence technology, more and more scholars are applying deep neural networks to describe the nonlinear motion state of the surrounding vehicles. Optical flow can be defined as the movement of an object between consecutive frames of a video sequence as a result of the relative motion between the object and the camera. Some researchers designed neural networks based on the optical flow characteristics in the appearance features to describe the motion correlation of the tracked vehicle [170], [171], [172]. In order to better enable the network to learn feature similarities between targets, high-order matching feature similarity measures were also introduced in [173]. Due to the powerful nonlinear modeling capability of deep neural networks (DNNs), some researchers constructed DNNs to directly describe the nonlinear motion states of target vehicles, such as multi ANNs [174] and MotionNet [175]. However, the performance of traditional NN-based methods is easily affected by the quality of training data, and the robustness of the algorithm under environmental interference cannot be guaranteed.

3) *V2X-Based Methods for Surrounding Vehicle State Estimation:* Existing autonomous vehicles are equipped with advanced perception sensors. However, the on-board perception sensors cannot reliably perceive in adverse weather conditions or when the perception sensors fail. In recent years, the development of V2X communication technology further improved the accuracy of surrounding vehicle state estimation.

Most of the existing cooperative vehicle tracking algorithms assume that the self-positioning information of the host vehicle and other connected vehicles is accurate. However, in dense urban environments, the positioning information provided by GPS may not be reliable. For this reason, some methods considering the time-varying noise uncertainty of relative positioning were proposed in [176] and [177]. Due to the better adaptability of roadside LiDAR compared to visual sensors in highly occluded scenes, a correlation method based on a search process and micro-motion model was designed in [178].

Considering the importance of lateral states such as lateral velocity and yaw rate in accurately describing the motion state of surrounding vehicles, the visual perception system of the host vehicle can provide the lateral offset and heading angle of the preceding vehicle. The traditional in-vehicle sensors in the preceding vehicle can measure the steering angle and yaw rate, and then transmit them to the host vehicle through V2V communication. However, the low communication transmission rate of V2V could affect the accuracy of the obtained state variables. To address this issue, various methods were proposed to conduct preliminary explorations on this, such as the information matrix filter [179] and cascaded KF [180]. To further address the negative impact of communication delay and data loss on the estimation method in the V2X environment, an event-triggered CKF algorithm was proposed to balance prediction accuracy and transmission rate, reducing the impact of data packet loss on estimation accuracy [181]. Similar studies were conducted in [182] and [183].

B. Surrounding Pedestrian State Estimation

In heterogeneous traffic, pedestrians and cyclists are vulnerable. Accurate estimation of the state of pedestrians and cyclists is crucial for the traffic safety of intelligent transportation systems. This is another challenging research topic. Cyclists and pedestrians use crosswalks at intersections, sidewalks, or non-motorized lanes on nearby roads. However, some pedestrians and cyclists break traffic laws and act unexpectedly, which can cause accidents. It is necessary to estimate their motion states because intelligent transportation system perception sensors might fail to directly measure such dangerous actions. Depending on whether a physical motion model of the object is established, mainstream pedestrian tracking object localization methods can be divided into physics model-based and deep learning-based approaches.

In the physical model-based methods, similarly to the surrounding vehicles, the filter-based methods were also widely used for pedestrian localization, such as KP-based methods [184], [185], [186], [187], EKF-based methods [188], UKF-based methods [189], [190], particle filter-based methods [191], [192], [193], [194]. In addition, to further improve the robustness of the algorithm, the pedestrian social force model [195] and IMM theory [196] were also applied to the design of pedestrian tracking algorithms. To address performance degradation in specific scenarios, scholars advocated a fusion approach leveraging multiple sensors, such as radar with monocular cameras [197], [198] and cameras with LiDAR [199], capitalizing on their strengths in accuracy.

One of the challenges in tracking problems is noise or occlusion. Physics model-based methods are often sensitive to measurement noise and lose track when the target is occluded for a while. To address these issues, deep learning techniques were also widely applied to the estimation of motion states for surrounding pedestrians. Considering traffic safety, human drivers prioritize their attention on nearby targets, meaning that closer vulnerable road users should receive more attention. Therefore, some researchers considered adding attention mechanisms into network designs, such as the dual-attention

network [200], HRNet with the polarized self-attention [201], one-stage network with coordinate attention mechanism [202].

C. Emerging State Estimation Methods for Surrounding Vehicles and Pedestrians

Due to the effectiveness of Transformer-based methods in handling long sequences and large-scale data in the field of natural language processing, this emerging technology has also garnered significant attention in multi-object tracking. Compared with traditional NNs, Transformers leverage the self-attention mechanism to focus computational power or gradient updates on crucial components to easily capture global dependencies [203].

A semantic segmentation network was integrated into the Transformer architecture to extract the foreground from input images, enabling the Transformer to focus more attention on the foreground and thereby enhance performance [204]. A tracking architecture called TransCenter was introduced in [205], utilizing dense representations within a Transformer framework. This proposed approach is capable of maintaining high tracking accuracy even in highly crowded and dense environments. To alleviate the issue of target occlusion encountered by vision-based methods, an autoregressive graph Transformer [206] was proposed to achieve more robust tracking results. To simultaneously capture the spatial-temporal information of targets, similar studies were also reported in [207], [208], and [209].

Based on LiDAR point cloud data, Ding et al. [210] designed a graph-based 3D multi-object tracking framework built upon the Transformer architecture, and proposed a novel autoregressive forward propagation and sequential mini-batch optimization training strategy to enhance model generalization. To recover objects missed by detectors, multiple trajectory hypotheses were generated [211], which can propagate the historical trajectory information of objects to the current frame. Moreover, anchor points extracted from the scene point cloud were used as object queries to balance accuracy and efficiency [212]. The integration of multi-modal sensor information with the Transformer architecture has also proved to be an effective method to enhance performance [213].

Hybrid methods that combine deep learning techniques with traditional physical models are generally considered to improve the interpretability of the framework and introduce physical constraints, thereby enhancing the reliability of tracking results. A classical optical flow estimation method based on the pyramidal Lucas-Kanade algorithm was effectively embedded into a deep learning-based multi-object tracking framework [214]. Li et al. [215] proposed a framework for simultaneous object tracking and prediction, where a learning-based prediction model served as an alternative to the traditional physical motion model. A kinematics model layer was introduced to enhance the physical feasibility of the learning-based motion model.

Physics model-based methods are sensitive to sensor noise and often rely on assumptions of constant velocity and constant acceleration. As a result, they may not perform well in estimating the motion states of pedestrians in scenarios with

TABLE X
RELATED PUBLIC DATASETS FOR THE STATE ESTIMATION OF VEHICLE-ROAD-PEDESTRIAN

| Datasets | Year | Sensors | Scenarios | Frames | RS | SVP |
|----------|------|---------|-----------|--------|-----|-----|
| KITTI | 2012 | C/L | U/C/H | 19,103 | < | |
| MOT17 | 2017 | C | U | 11,235 | < | |
| MOT20 | 2020 | C | U | 13,410 | < | |
| NuScenes | 2020 | C/R/L | U | 40,157 | < | |
| BDDIOOK | 2020 | C | U | 12e7 | * | |
| RoadSaW | 2022 | C/M | U/H | 72e4 | ** | < |
| RSCD | 2022 | C | U/C/H | 103e4 | *** | < |
| WRF | 2022 | C | U/H | 5,061 | *** | < |
| RSRD | 2023 | C/L | U/C | 16,000 | | < |

¹ RS: road surface; SVP: surrounding vehicles and pedestrians; In "Sensors", C: camera, R: radar, L: LiDAR, M: mobile advanced road weather information sensor; In "Scenarios", U: urban, C: countryside, H: highway.

² *including snowy/icy road surface; **including the annotation of road surface condition; ***including both of the above.

sudden behavior changes or dense occlusions. In comparison, deep learning-based methods can handle abrupt intention changes in pedestrian motion state estimation. However, they are susceptible to the quality of training data and may produce unreasonable estimation results. The deployment issue on edge computing platforms with limited computing power still needs further consideration. Therefore, considering that the existing research on physics-informed hybrid methods is still very limited, the state estimation of surrounding traffic participants combining physical models and deep learning techniques is still worthy of further exploration.

VI. PERFORMANCE EVALUATION

Due to the site limitations and potential safety risks associated with direct real-vehicle testing, simulation platforms greatly promote the development of state estimation algorithms. Moreover, high-quality datasets are the important driving forces to improve the performance of learning-based estimation methods. This section summarizes the open-source datasets and experiment platforms used in the literature.

A. Datasets

The accuracy and generalization of data-driven methods depend on dataset size and quality. While the autonomous driving community has many public datasets, this paper summarizes those relevant to intelligent transportation system dynamic state estimation, including publication year, sensor configurations, data scale, and task-related details. TABLE X summarizes related public datasets.

Existing famous public datasets for autonomous driving, such as the KITTI [216], BDDIOOK [217], MOT17/MOT20 [218], and NuScenes [219] datasets, primarily focus on the road traffic participants and do not specifically address the estimation of road surface states. However, the information about road surface states is crucial for the traffic safety of intelligent transportation systems. Consequently, some researchers developed relevant datasets to address this gap, such as WRF [115], RoadSaW [116], RSCD [114], and RSRD [147], [220] for road unevenness perception of autonomous driving.

TABLE XI
COMPARISON OF EVALUATION METRICS FOR ESTIMATION ACCURACY

| Metrics | S.O. | Applicable scenarios |
|---------|------|---|
| RMSE | +++ | 1) Available in most estimation algorithms; 2) Applicable for situations where the large error of estimation results need to be sensitively reflected |
| MAE | ++ | Applicable for measuring overall estimated performance that requires disregarding large estimation errors |
| CA | + | Applicable in classification algorithms (e.g., learning-based estimation methods) |

¹ S.O.: sensitivity to outliers; RMSE: root mean squared error; MAE: mean absolute error; CA: Top-1 classification accuracy; "+" low; "++": moderate; "+++": high.

B. Metrics

This subsection summarizes the evaluation metrics related to the state estimation methods. Since the evaluation metrics for object tracking are used to evaluate the overall performance of the tracking algorithms, they are not within the scope discussed in this paper. The comparison of summarized evaluation metrics for estimation accuracy is listed in TABLE XI.

1) *Root Mean Squared Error*: Root mean squared error (RMSE) is a common metric used to quantify the discrepancy between estimated values and reference values. The calculation formula for RMSE [24] is as follow:

$$RMSE = \sqrt{\frac{1}{n} \sum_{t=1}^n (\mathbf{e}_{(t)} - e_{ref}(t))^2}, \quad (2)$$

where n is the total number of samples within a certain period, the estimation result $\mathbf{e}_{(t)}$ at time t , and $e_{ref}(t)$ is the reference true value at time t .

2) *Mean Absolute Error*: Mean absolute error (MAE) [51] measures the average absolute error between the estimated value and the actual value:

$$MAE = \frac{1}{n} \sum_{t=1}^n |\mathbf{e}_{(t)} - e_{ref}(t)|. \quad (3)$$

3) *Top-1 Classification Accuracy*: Top-1 classification accuracy [114] is a widely used evaluation metric in machine learning, particularly for image classification tasks. The model's top-ranked prediction should be the same as the true label for a sample. If the model predicts the correct class as the top choice, it is counted as a correct prediction. Top-1 accuracy is determined by dividing the number of correct predictions by the total number of samples in the test dataset.

4) *Convergence Time*: The convergence time of an estimation algorithm is one of the crucial metrics for evaluating algorithm performance [31]. It measures the time required for an estimation algorithm to reach the convergence state from the beginning of its execution. A slower convergence time may lead to the algorithm's inability to meet real-time requirements or cause significant computational delays in practice.

5) *Computation Time*: Due to the limitations of the on-board computing platform, shorter calculation time means that the algorithm can release computing resources faster for other algorithm modules [33]. In addition, the decision-making

TABLE XII

SIMULATION EXPERIMENT PLATFORMS FOR THE STATE ESTIMATION OF VEHICLE-ROAD-PEDESTRIAN

| Software | Year | TSC | VDC | O.S. | GRR | References |
|------------|------|-----|-----|------|-----|-------------|
| CarSim | 1990 |)< | +++ |)< | + | [34], [181] |
| TruckSim | 1990 |)< | +++ |)< | + | [37] |
| PTV-VISSIM | 1992 | +++ |)< |)< | +++ | [130] |
| AIMSUN | 1997 | +++ |)< |)< | +++ | [124] |
| PreScan | 2004 | ++ | ++ |)< | +++ | [87] |
| DYNA4 | 2010 | + | ++ |)< | ++ | [125] |
| SUMO | 2011 | +++ |)< | .I | ++ | [221] |
| MSC VTD | 2017 | ++ | ++ |)< | +++ | [222] |
| CARLA | 2017 | ++ |)< | .I | +++ | [223] |
| MATLAB ADT | 2017 | + | + |)< | ++ | [161] |

¹TSC: traffic scene configuration; VDC: vehicle dynamics configuration; O.S.: open-source; GRR: graphics rendering requirements; MATLAB ADT: MATLAB automated driving toolbox; MSC VTD: MSC Virtual Test Drive; "+": low; "++": moderate; "+++": high.

and planning system of autonomous vehicles uses state estimation results to achieve safe and efficient driving, thereby improving the system's adaptability to dynamic environmental changes.

C. Experiment Platform

During the development and validation phases of estimation algorithms, researchers commonly utilize experimental platforms to evaluate performance. By simulating diverse driving scenarios and conditions, they can assess an algorithm's accuracy, stability, and overall effectiveness. This process ensures that the algorithm is well-prepared for real-world deployment and widespread application.

1) *Simulation Platform*: Experiments based on real vehicles usually have potential safety risks. The simulation experiment is one of the most important methods to verify algorithm performance. It can verify the performance of algorithms in as many scenarios as possible in a safe and low-cost manner. The summary of related simulation experiment platforms is shown in TABLE XII. As for the vehicle dynamics simulation platform, CarSim [34] is a physics-based simulation software platform used for simulating and evaluating vehicle dynamics and driving characteristics. Additionally, CarSim can simulate various driving scenarios, road conditions, and environmental factors, including wet and slippery surfaces, cornering maneuvers, and emergency braking. TruckSim [37] is a widely used tool in the field of truck engineering and development. Regarding the construction and simulation of common traffic scenarios, there are several common platforms for generating realistic traffic flows, such as PTV-VISSIM [130], AIMSUN [124], and SUMO [221]. It is worth noting that the following software can be co-simulated with CarSim or TruckSim, such as PreScan [87], MSC VTD [222], CARLA [223], and MATLAB Automated Driving Toolbox [161].

2) *Physical Platform*: In the simulation experiment, the noise disturbance in the simulation environment is relatively small compared with the real world, and the robustness of the algorithm cannot be further evaluated. In order to better evaluate the performance of the estimation algorithm when

TABLE XIII

PHYSICAL EXPERIMENT PLATFORM FOR THE STATE ESTIMATION OF VEHICLE-ROAD-PEDESTRIAN

| State | Type | IVS | P.S. | ECU | GPU | V2X | GT | Ref. |
|-------|------|-----|--------|-----|-----|-----|-------------|-------|
| EVSA | ONR | .I |)< | .I |)< |)< | DGPS | [34] |
| | ONR | .I |)< | .I |)< |)< | S-Motion | [52] |
| | HIL | .I |)< | .I |)< |)< | TruckSim | [37] |
| | TRFC | ONR | .I |)< | .I |)< | Transducer | [88] |
| | HIL | .I |)< | .I |)< |)< | CarSim | [94] |
| | ONR |)< | Camera |)< | .I |)< | E.V. | [114] |
| SVPS | ONR |)< | LiDAR |)< | .I |)< | Grip tester | [117] |
| | ONR | .I | Camera | .I | .I |)< | Pendulum | [121] |
| | ONR |)< | LiDAR | .I | .I |)< | GNSS | [159] |
| | ONR |)< | LiDAR |)< | .I |)< | GNSS | [161] |
| | ONR | .I |)< | .I |)< | .I | GNSS | [181] |

¹ IVS: in-vehicle sensors; P.S.: perception sensors; ECU: electronic control unit; GPU: graphics processing unit; GT: ground truth; DGPS: differential GPS; E.V.: empirical value.

² EVSA: ego-vehicle sideslip angle; SVPS: surrounding vehicle and pedestrian states; HIL: hardware-in-loop; ONR: on-road test.

applied in real-world environments, physical experimental verification is essential. The summary of physical experiment platforms is shown in TABLE XIII. The schematic diagram of the physical experiment platforms is presented in Fig. 13.

As shown in Fig. 13, the hardware components of a hardware-in-loop (HIL) testing platform are mainly as follows: 1) an ECU that executes the onboard estimation algorithm; 2) a host computer that can configure precise vehicle models and perform data logging and calibration via the CAN software; 3) a secondary computer that mainly runs the compiled high-fidelity vehicle model from the host computer and exports real-time vehicle response signals to the ECU; 4) an in-loop actuator that generates actuator signals.

The test platform for on-road tests (ONR) mainly consists of the following components: 1) A test vehicle with high-precision measuring instruments provides vehicle response signals and reference values of estimated states. 2) Perception sensors can capture information about surrounding traffic participants and the road surface. 3) An onboard computer with GPUs is responsible for real-time data processing from perception sensors. 4) A rapid control prototyping (RCP) serves as an ECU that executes onboard estimation algorithms. Compared to a standard onboard ECU, the main advantage of RCP is to adjust model parameters in real-time during testing without recompiling and downloading the code.

VII. CHALLENGES AND FUTURE PERSPECTIVES

From the review of the literature, the existing dynamic state estimation methods for vehicle-road-pedestrian primarily focus on physics model-based and learning-based approaches. While significant progress has been made in these areas, there are still several challenges that need to be addressed. The following is a summary of the challenges and research directions for future studies as shown in Fig. 14.

1) *Robust State Estimation With Model Uncertainty*: State estimation for vehicle-road-pedestrian needs to address significant system coupling issues. In particular, when tire models

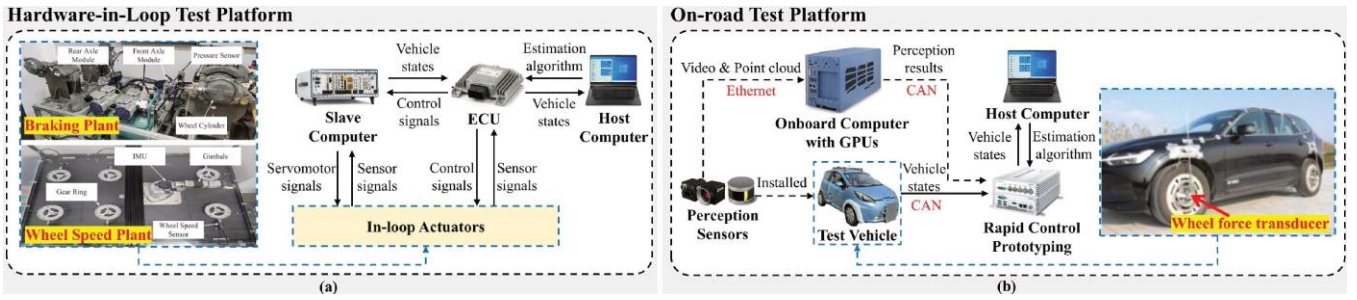


Fig. 13. Schematic diagram of typical physical experiment platforms. (a) Hardware-in-loop test platform [37]; (b) On-road test platform [88].

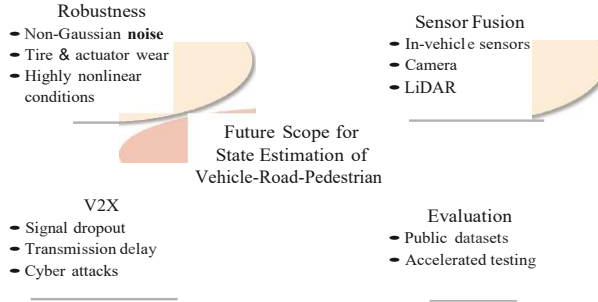


Fig. 14. Illustration of future research directions.

and vehicle dynamic models are subjected to highly nonlinear and complex excitation conditions, the model parameters exhibit strong nonlinear and time-varying characteristics, leading to slow convergence of the estimator. Taking TRFC estimation as an example, dynamics model-based state estimation methods heavily rely on the accuracy of tire modeling. As the vehicle mileage increases, the tire may inevitably experience wear, resulting in changes to the tire model parameters and affecting the estimation accuracy of algorithms that are based on the original tire model parameter. Additionally, most existing estimation methods assume ideal Gaussian noise distributions for modeling, but in real-world environments, sensor noise often exhibits non-Gaussian characteristics. It is also worth studying the impact of unpredictable interactions between traffic participants on the robustness of the estimation algorithm. Hence, designing distributed robust state estimation algorithms considering model parameter uncertainty and noise variability is an exploratory direction.

2) Multimodal State Estimation With Environmental Interference: Existing state estimation methods often rely on idealized assumptions regarding normal weather conditions. The non-ideal environmental conditions, such as building occlusions, poor lighting, and adverse weather conditions like rain or snow, can severely impact the normal functioning of environmental perception sensors. With an increasing number of intelligent vehicles equipped with LiDAR, the robustness of LiDAR point cloud information against environmental light variations makes LiDAR-based state estimation methods essential for expanding the application scenarios of estimation algorithms. Therefore, investigating multimodal state estimation methods considering complex environmental factors is necessary.

3) Fault-Tolerant State Estimation Considering Signal Dropout and Cyberattacks: With the rapid development of V2X technology, the host vehicle can not only communicate with other vehicles (V2V) but also interact with roadside infrastructure (V2I). Roadside units can share information about road conditions or the motion states of surrounding traffic participants with the host vehicle based on historical data. They can also obtain the key state information of vehicle-road-pedestrian regarding the current driving conditions through communication with other vehicles. However, the estimation accuracy of V2X-based methods may be limited by the precision and measurement performance of certain sensors. On the one hand, some sensors may experience failures due to aging or extreme weather conditions. Some researchers have already explored estimation methods that take into account communication delays or signal dropout [26], [27], [29], [89], as well as asynchronously sampled measurements [224]. Nevertheless, there is still a need for further research. On the other hand, traditional communication devices are vulnerable to cyberattacks. The above problems may seriously degrade the estimation performance of normal V2X-based state estimation methods [225], [226]. Therefore, it is necessary to consider designing fault-tolerant state estimation methods considering signal dropout and cyberattacks.

4) Effective Public Evaluation Platform: Although there are large-scale image datasets available for road surface condition classification, there is still a lack of an effective evaluation platform for existing estimation methods. The main function of this platform should be to use a small number of test maneuvers to reflect the performance of the algorithm in most working conditions to achieve accelerated testing [227]. This lack can make it difficult to evaluate and compare various estimation methods. Consequently, it is necessary to establish an effective public evaluation platform.

VIII. CONCLUSION

In this survey, based on the systemwide perspective of ITS, a specific perspective of "vehicle-road-pedestrian" is adopted to comprehensively review the state estimation methods for the above traffic elements in recent years. It is shown that the majority of the existing state estimation methods for "vehicle-road-pedestrian" focus on either physics models or machine learning. Physics model-based estimation methods offer advantages, such as easy deployment and low computational burden but are susceptible to modeling accuracy and

sensor noise. Machine learning-based estimation methods can handle nonlinear mappings for complex conditions but are sensitive to external environmental factors and the quality of training data. Therefore, fault-tolerant estimation methods that leverage multi-source sensor information and integrate V2X technology are promising research directions. Additionally, this survey provides a detailed summary of relevant datasets, evaluation metrics, and experimental platforms in this field. However, it is noted that the challenges for the performance evaluation remain, including the limited availability of public datasets, and a lack of effective evaluation scenarios and testing platforms. Due to the length limit, we excluded a detailed review of vehicle mass estimation, road slope estimation, and TRFC estimation based on intelligent tire sensors. The summary of recent trends in tire-road interaction estimation based on intelligent tires can be found in [228]. In addition, a detailed review of the trajectory prediction of surrounding traffic participants in downstream tasks of the state estimation is also beyond the scope of this survey. The relevant emerging technologies mainly include Transformer, generative adversarial networks (GANs), and variational autoencoders (VAEs) [229], [230]. The generator of GANs learns from historical trajectories to generate future trajectories, while the discriminator evaluates the realism of the generated trajectories.

Despite the valuable research progress achieved in this field, various challenges still exist. It is expected that this survey can facilitate the application and deployment of the mentioned research in ITS and promote further advancement in future research directions discussed in this survey.

REFERENCES

- [1] A. Eskandarian, C. Wu, and C. Sun, "Research advances and challenges of autonomous and connected ground vehicles," *IEEE Trans. Intel./. Transp. Syst.*, vol. 22, no. 2, pp. 683-711, Feb. 2021.
- [2] J. Wu, C. Huang, H. Huang, C. Lv, Y. Wang, and F.-Y. Wang, "Recent advances in reinforcement learning-based autonomous driving behavior planning: A survey," *Transp. Res. C, Emerg. Technol.*, vol. 164, Jul. 2024, Art. no. 104654.
- [3] B. Chen, D. Sun, J. Zhou, W. Wong, and Z. Ding, "A future intelligent traffic system with mixed autonomous vehicles and human-driven vehicles," *Inf. Sci.*, vol. 529, pp. 59-72, Aug. 2020.
- [4] P. Ghorai, A. Eskandarian, Y.-K. Kim, and G. Mehr, "State estimation and motion prediction of vehicles and vulnerable road users for cooperative autonomous driving: A survey," *IEEE Trans. Intel./. Transp. Syst.*, vol. 23, no. 10, pp. 16983-17002, Oct. 2022.
- [5] M. Pechinger, G. Schroer, K. Bogenberger, and C. Markgraf, "Roadside infrastructure support for urban automated driving," *IEEE Trans. Intel./. Transp. Syst.*, vol. 24, no. 10, pp. 10643-10652, Oct. 2023.
- [6] Z. MacHardy, A. Khan, K. Obana, and S. Iwashina, "V2X access technologies: Regulation, research, and remaining challenges," *IEEE Commun. Surveys Tuts.*, vol. 20, no. 3, pp. 1858-1877, 3rd Quart., 2018.
- [7] Y. Wang et al., "Self-learning control for coordinated collision avoidance of automated vehicles," *Proc. Inst. Mech. Eng. D, J. Automobile Eng.*, vol. 235, no. 4, pp. 1149-1163, Mar. 2021.
- [8] F. J. Belmonte, S. Martin, E. Sanristobal, J. A. Ruiperez-Valiente, and M. Castro, "Overview of embedded systems to build reliable and safe ADAS and AD systems," *IEEE Intel./. Transp. Syst. Mag.*, vol. 13, no. 4, pp. 239-250, Winter. 2021.
- [9] Z. Li, J. Hu, B. Leng, L. Xiong, and Z. Fu, "An integrated decision making and motion planning framework for enhanced oscillation-free capability," *IEEE Trans. Intel./. Transp. Syst.*, vol. 25, no. 6, pp. 5718-5732, Jun. 2024.
- [10] H. Yang, H. Liu, Z. Hu, A.-T. Nguyen, T.-M. Guerra, and C. Lv, "Quantitative identification of driver distraction: A weakly supervised contrastive learning approach," *IEEE Trans. Intel./. Transp. Syst.*, vol. 25, no. 2, pp. 2034-2045, Feb. 2024.
- [11] H. Yang, J. Wu, Z. Hu, and C. Lv, "Real-time driver cognitive workload recognition: Attention-enabled learning with multimodal information fusion," *IEEE Trans. Ind. Electron.*, vol. 71, no. 5, pp. 4999-5009, May 2024.
- [12] X. Xia et al., "Estimation on IMU yaw misalignment by fusing information of automotive onboard sensors," *Mech. Syst. Signal Process.*, vol. 162, Jan. 2022, Art. no. 107993.
- [13] W. Liu et al., "A systematic survey of control techniques and applications in connected and automated vehicles," *IEEE Internet Things J.*, vol. 10, no. 24, pp. 21892-21916, Dec. 2023.
- [14] H. Guo, Z. Yin, D. Cao, H. Chen, and C. Lv, "A review of estimation for vehicle tire-road interactions toward automated driving," *IEEE Trans. Syst., Man, Cybern., Syst.*, vol. 49, no. 1, pp. 14-30, Jan. 2019.
- [15] Z. Sun, J. Chen, L. Chao, W. Ruan, and M. Mukherjee, "A survey of multiple pedestrian tracking based on tracking-by-detection framework," *IEEE Trans. Circuits Syst. Video Technol.*, vol. 31, no. 5, pp. 1819-1833, May 2021.
- [16] S. Ansari, F. Naghd, and H. Du, "Human-machine shared driving: Challenges and future directions," *IEEE Trans. Intel./. Vehicles*, vol. 7, no. 3, pp. 499-519, Sep. 2022.
- [17] H. Guo, D. Cao, H. Chen, C. Lv, H. Wang, and S. Yang, "Vehicle dynamic state estimation: State of the art schemes and perspectives," *IEEE/CAA J. Autom. Sinica*, vol. 5, no. 2, pp. 418-431, Mar. 2018.
- [18] K. B. Singh, M. A. Arat, and S. Taheri, "Literature review and fundamental approaches for vehicle and tire state estimation," *Vehicle Syst. Dyn.*, vol. 57, no. 11, pp. 1643-1665, Nov. 2019.
- [19] W. Luo, J. Xing, A. Milan, X. Zhang, W. Liu, and T.-K. Kim, "Multiple object tracking: A literature review," *Artif. Intel./.*, vol. 293, Apr. 2021, Art. no. 103448.
- [20] Y. Wang et al., "Tire road friction coefficient estimation: Review and research perspectives," *Chin. J. Mech. Eng.*, vol. 35, no. 1, pp. 1-11, Dec. 2022.
- [21] Y. Wang, H. Wei, L. Yang, B. Hu, and C. Lv, "A review of dynamic state estimation for the neighborhood system of connected vehicles," *SAE Int. J. Vehicle Dyn., Stability, NVH*, vol. 7, no. 3, pp. 367-385, Jul. 2023.
- [22] L. Xiong et al., "IMU-based automated vehicle slip angle and attitude estimation aided by vehicle dynamics," *Sensors*, vol. 19, no. 8, p. 1930, Apr. 2019.
- [23] X. Jin, J. Yang, L. Xu, C. Wei, Z. Wang, and G. Yin, "Combined estimation of vehicle dynamic state and inertial parameter for electric vehicles based on dual central difference Kalman filter method," *Chin. J. Mech. Eng.*, vol. 36, no. 1, pp. 1-16, Aug. 2023.
- [24] Y.-W. Liao and F. Borrelli, "An adaptive approach to real-time estimation of vehicle sideslip, road bank angles, and sensor bias," *IEEE Trans. Veh. Technol.*, vol. 68, no. 8, pp. 7443-7454, Aug. 2019.
- [25] X. Li, N. Xu, Q. Li, K. Guo, and J. Zhou, "A fusion methodology for sideslip angle estimation on the basis of kinematics-based and model-based approaches," *Proc. Inst. Mech. Eng. D, J. Automobile Eng.*, vol. 234, no. 7, pp. 1930-1943, 2020.
- [26] Y. Wang, L. Xu, F. Zhang, H. Dong, Y. Liu, and G. Yin, "An adaptive fault-tolerant EKF for vehicle state estimation with partial missing measurements," *IEEE/ASM E Trans. Mechatronics*, vol. 26, no. 3, pp. 1318-1327, Jun. 2021.
- [27] H. Yuan and X. Song, "A modified EKF for vehicle state estimation with partial missing measurements," *IEEE Signal Process. Lett.*, vol. 29, pp. 1594-1598, 2022.
- [28] L. Mosconi, F. Farroni, A. Sakhnevych, F. Timpone, and F. S. Gerbino, "Adaptive vehicle dynamics state estimator for onboard automotive applications and performance analysis," *Vehicle Syst. Dyn.*, vol. 61, no. 12, pp. 3244-3268, Dec. 2023.
- [29] Y. Wang, H. Wei, B. Hu, and C. Lv, "Robust estimation of vehicle dynamic state using a novel second-order fault-tolerant extended Kalman filter," *SAE Int. J. Vehicle Dyn., Stability, NVH*, vol. 7, no. 3, pp. 301-311, May 2023.
- [30] D. Qi, J. Feng, X. Ni, and L. Wang, "Maximum correntropy extended Kalman filter for vehicle state observation," *Int. J. Automot. Technol.*, vol. 24, no. 2, pp. 377-388, Apr. 2023.
- [31] X. Ping, S. Cheng, W. Yue, Y. Du, X. Wang, and L. Li, "Adaptive estimations of tyre-road friction coefficient and body's sideslip angle based on strong tracking and interactive multiple model theories," *Proc. Inst. Mech. Eng. D, J. Automobile Eng.*, vol. 234, no. 14, pp. 3224-3238, Dec. 2020.
- [32] Z. Xue, S. Cheng, L. Li, Z. Zhong, and H. Mu, "A robust unscented M-estimation-based filter for vehicle state estimation with unknown input," *IEEE Trans. Veh. Technol.*, vol. 71, no. 6, pp. 6119-6130, Jun. 2022.

- [33] Y. Zhang, M. Li, Y. Zhang, Z. Hu, Q. Sun, and B. Lu, "An enhanced adaptive unscented Kalman filter for vehicle state estimation," *IEEE Trans. Instrum. Meas.*, vol. 71, pp. 1-12, 2022.
- [34] Y. Wang, K. Geng, L. Xu, Y. Ren, H. Dong, and G. Yin, "Estimation of sideslip angle and tire cornering stiffness using fuzzy adaptive robust cubature Kalman filter," *IEEE Trans. Syst., Man, Cybern., Syst.*, vol. 52, no. 3, pp. 1451-1462, Mar. 2022.
- [35] L. Yarning, Z. Kongyun, S. Peicheng, Z. Linfeng, F. Yongle, and D. Yufeng, "Distributed electric vehicle state parameter estimation based on the ASO-SRGHCKF algorithm," *IEEE Sensors J.*, vol. 22, no. 19, pp. 18780-18792, Oct. 2022.
- [36] T. Chen, Y. Cai, L. Chen, and X. Xu, "Sideslip angle fusion estimation method of three-axis autonomous vehicle based on composite model and adaptive cubature Kalman filter," *IEEE Trans. Transport. Electricific.*, vol. 10, no. 1, pp. 316-330, Mar. 2023.
- [37] Y. Liu, C. Huang, D. Zhou, X. Wang, and L. Li, "Vehicle sideslip angle estimation based on strong tracking SCKF considering road inclinations," *IEEE Trans. Veh. Technol.*, vol. 72, no. 12, pp. 15535-15547, Dec. 2023.
- [38] W. Zhang, Z. Wang, C. Zou, L. Drugge, and M. Nybacka, "Advanced vehicle state monitoring: Evaluating moving horizon estimators and unscented Kalman filter," *IEEE Trans. Veh. Technol.*, vol. 68, no. 6, pp. 5430-5442, Jun. 2019.
- [39] A.-T. Nguyen, T.-M. Guerra, C. Sentouh, and H. Zhang, "Unknown input observers for simultaneous estimation of vehicle dynamics and driver torque: Theoretical design and hardware experiments," *IEEE/ASME Trans. Mechatronics*, vol. 24, no. 6, pp. 2508-2518, Dec. 2019.
- [40] M. Fouka, C. Sentouh, and J.-C. Popieul, "Quasi-LPV interconnected observer design for full vehicle dynamics estimation with hardware experiments," *IEEE/ASME Trans. Mechatronics*, vol. 26, no. 4, pp. 1763-1772, Aug. 2021.
- [41] A.-T. Nguyen, T. Q. Dinh, T.-M. Guerra, and J. Pan, "Takagi-Sugeno fuzzy unknown input observers to estimate nonlinear dynamics of autonomous ground vehicles: Theory and real-time verification," *IEEE/ASME Trans. Mechatron.*, vol. 26, no. 3, pp. 1328-1338, Jun. 2021.
- [42] W. Li, Z. Xie, P.K. Wong, Y. Hu, G. Guo, and J. Zhao, "Event-triggered asynchronous fuzzy filtering for vehicle sideslip angle estimation with data quantization and dropouts," *IEEE Trans. Fuzzy Syst.*, vol. 30, no. 8, pp. 2822-2836, Aug. 2022.
- [43] Q. Zhang, H. Jing, Z. Liu, Y. Jiang, and M. Gu, "A novel PWA lateral dynamics modeling method and switched T-S observer design for vehicle sideslip angle estimation," *IEEE Trans. Ind. Electron.*, vol. 69, no. 2, pp. 1847-1857, Feb. 2022.
- [44] B. L. Boada, F. Viadero-Monasterio, H. Zhang, and M. J. L. Boada, "Simultaneous estimation of vehicle sideslip and roll angles using an integral-based event-triggered H_{∞} observer considering intravehicle communications," *IEEE Trans. Veh. Technol.*, vol. 72, no. 4, pp. 4411-4425, Apr. 2023.
- [45] A. Leanza, G. Mantriota, and G. Reina, "On the vehicle dynamics prediction via model-based observation," *Vehicle Syst. Dyn.*, vol. 62, no. 5, pp. 1181-1202, May 2024.
- [46] L. Xiong et al., "IMU-based automated vehicle body sideslip angle and attitude estimation aided by GNSS using parallel adaptive Kalman filters," *IEEE Trans. Veh. Technol.*, vol. 69, no. 10, pp. 10668-10680, Oct. 2020.
- [47] W. Liu, X. Xia, L. Xiong, Y. Lu, L. Gao, and Z. Yu, "Automated vehicle sideslip angle estimation considering signal measurement characteristic," *IEEE Sensors J.*, vol. 21, no. 19, pp. 21675-21687, Oct. 2021.
- [48] X. Xia, E. Hashemi, L. Xiong, A. Khajepour, and N. Xu, "Autonomous vehicles sideslip angle estimation: Single antenna GNSS/IMU fusion with observability analysis," *IEEE Internet Things J.*, vol. 8, no. 19, pp. 14845-14859, Oct. 2021.
- [49] X. Xia, L. Xiong, Y. Lu, L. Gao, and Z. Yu, "Vehicle sideslip angle estimation by fusing inertial measurement unit and global navigation satellite system with heading alignment," *Mech. Syst. Signal Process.*, vol. 150, Mar. 2021, Art. no. 107290.
- [50] X. Ding, Z. Wang, and L. Zhang, "Event-triggered vehicle sideslip angle estimation based on low-cost sensors," *IEEE Trans. Ind. Informal.*, vol. 18, no. 7, pp. 4466-4476, Jul. 2022.
- [51] Z. Zhang, J. Zhao, C. Huang, and L. Li, "Precise and robust sideslip angle estimation based on INS/GNSS integration using invariant extended Kalman filter," *Proc. Inst. Mech. Eng. D, J. Automobile Eng.*, vol. 237, no. 8, pp. 1805-1818, Jul. 2023.
- [52] X. Xia, P. Hang, N. Xu, Y. Huang, L. Xiong, and Z. Yu, "Advancing estimation accuracy of sideslip angle by fusing vehicle kinematics and dynamics information with fuzzy logic," *IEEE Trans. Veh. Technol.*, vol. 70, no. 7, pp. 6577-6590, Jul. 2021.
- [53] R. Song and Y. Fang, "Vehicle state estimation for INS/GPS aided by sensors fusion and SCKF-based algorithm," *Mech. Syst. Signal Process.*, vol. 150, Mar. 2021, Art. no. 107315.
- [54] G. Park, "Vehicle sideslip angle estimation based on interacting multiple model Kalman filter using low-cost sensor fusion," *IEEE Trans. Veh. Technol.*, vol. 71, no. 6, pp. 6088-6099, Jun. 2022.
- [55] S. Rafatnia and M. Mirzaei, "Estimation of reliable vehicle dynamic model using IMU/GNSS data fusion for stability controller design," *Mech. Syst. Signal Process.*, vol. 168, Apr. 2022, Art. no. 108593.
- [56] L. Gao, L. Xiong, X. Xia, Y. Lu, Z. Yu, and A. Khajepour, "Improved vehicle localization using on-board sensors and vehicle lateral velocity," *IEEE Sensors J.*, vol. 22, no. 7, pp. 6818-6831, Apr. 2022.
- [57] X. Xia, E. Hashemi, L. Xiong, and A. Khajepour, "Autonomous vehicle kinematics and dynamics synthesis for sideslip angle estimation based on consensus Kalman filter," *IEEE Trans. Control Syst. Technol.*, vol. 31, no. 1, pp. 179-192, Jan. 2023.
- [58] W. Liu, L. Xiong, X. Xia, Y. Lu, L. Gao, and S. Song, "Vision-aided intelligent vehicle sideslip angle estimation based on a dynamic model," *JET Intell. Transp. Syst.*, vol. 14, no. 10, pp. 1183-1189, Oct. 2020.
- [59] A. Bonfitto, S. Feraco, A. Tonoli, and N. Amati, "Combined regression and classification artificial neural networks for sideslip angle estimation and road condition identification," *Vehicle Syst. Dyn.*, vol. 58, no. 11, pp. 1766-1787, Nov. 2020.
- [60] J. Liu, Z. Wang, L. Zhang, and P. Walker, "Sideslip angle estimation of ground vehicles: A comparative study," *JET Control Theory Appl.*, vol. 14, no. 20, pp. 3490-3505, Dec. 2020.
- [61] J. Liu, Z. Wang, and L. Zhang, "A time-delay neural network of sideslip angle estimation for in-wheel motor drive electric vehicles," in *Proc. IEEE 91st Veh. Technol. Conf. (VTC-Spring)*, May 2020, pp. 1-5.
- [62] S. Srinivasan, I. Sa, A. Zyner, V. Reijgwart, M. I. Valls, and R. Siegwart, "End-to-end velocity estimation for autonomous racing," *IEEE Robot. Autom. Lett.*, vol. 5, no. 4, pp. 6869-6875, Oct. 2020.
- [63] T. Novi, R. Capitani, and C. Annicchiarico, "An integrated artificial neural network-unscented Kalman filter vehicle sideslip angle estimation based on inertial measurement unit measurements," *Proc. Inst. Mech. Eng. D, J. Automobile Eng.*, vol. 233, no. 7, pp. 1864-1878, Jun. 2019.
- [64] C. Zhou, L. Yu, Y. Li, and J. Song, "Robust sideslip angle observer of commercial vehicles based on cornering stiffness estimation using neural network," *Proc. Inst. Mech. Eng. D, J. Automobile Eng.*, vol. 237, no. 1, pp. 224-243, Jan. 2023.
- [65] M. J. L. Boada, B. L. Boada, and H. Zhang, "Event-triggering H_{∞} -based observer combined with NN for simultaneous estimation of vehicle sideslip and roll angles with network-induced delays," *Nonlinear Dyn.*, vol. 103, no. 3, pp. 2733-2752, Feb. 2021.
- [66] C. M. Nguyen, A.-T. Nguyen, and S. Delprat, "Neural-network-based fuzzy observer with data-driven uncertainty identification for vehicle dynamics estimation under extreme driving conditions: Theory and experimental results," *IEEE Trans. Veh. Technol.*, vol. 72, no. 2, pp. 8686-8696, Jul. 2023.
- [67] D. Kim, K. Min, H. Kim, and K. Huh, "Vehicle sideslip angle estimation using deep ensemble-based adaptive Kalman filter," *Mech. Syst. Signal Process.*, vol. 144, Oct. 2020, Art. no. 106862.
- [68] R. Song, Y. Fang, and H. Huang, "Reliable estimation of automotive states based on optimized neural networks and moving horizon estimator," *IEEE/ASME Trans. Mechatronics*, vol. 28, no. 6, pp. 3238-3249, Dec. 2023.
- [69] B. Zhang, W. Zhao, S. Zou, H. Zhang, and Z. Luan, "A reliable vehicle lateral velocity estimation methodology based on SBI-LSTM during GPS-outage," *IEEE Sensors J.*, vol. 21, no. 14, pp. 15485-15495, Jul. 2021.
- [70] W. Jeon, A. Chakrabarty, A. Zemouche, and R. Rajamani, "Simultaneous state estimation and tire model learning for autonomous vehicle applications," *IEEE/ASME Trans. Mechatronics*, vol. 26, no. 4, pp. 1941-1950, Aug. 2021.
- [71] M. Viehweger et al., "Vehicle state and tyre force estimation: Demonstrations and guidelines," *Vehicle Syst. Dyn.*, vol. 59, no. 5, pp. 675-702, May 2021.
- [72] T. Gruber, S. Lupberger, M. Unterreiner, and D. Schramm, "A hybrid approach to side-slip angle estimation with recurrent neural networks and kinematic vehicle models," *IEEE Trans. Intell. Vehicles*, vol. 4, no. 1, pp. 39-47, Mar. 2019.

- [73] M. D. Lio, M. Piccinini, and F. Biral, "Robust and sample-efficient estimation of vehicle lateral velocity using neural networks with explainable structure informed by kinematic principles," *IEEE Trans. Intell. Transp. Syst.*, vol. 24, no. 12, pp. 13670-13684, Dec. 2023.
- [74] F. Dettu, S. Formentin, and S. Matteo Savaresi, "Joint vehicle state and parameters estimation via twin-in-the-loop observers," *Vehicle Syst. Dyn.*, vol. 62, no. 9, pp. 2423-2449, Sep. 2024.
- [75] Y. Song, H. Shu, X. Chen, and S. Luo, "Direct-yaw-moment control of four-wheel-drive electrical vehicle based on lateral tyre-road forces and sideslip angle observer," *JET Intell. Transp. Syst.*, vol. 13, no. 2, pp. 303-312, Feb. 2019.
- [76] H. Heidfeld, M. Schunemann, and R. Kasper, "UKF-based state and tire slip estimation for a 4WD electric vehicle," *Vehicle Syst. Dyn.*, vol. 58, no. 10, pp. 1479-1496, Oct. 2020.
- [77] Q. Wang, Y. Zhao, F. Lin, C. Zhang, and H. Deng, "Integrated control for distributed in-wheel motor drive electric vehicle based on states estimation and nonlinear MPC," *Proc. Inst. Mech. Eng. D, J. Automobile Eng.*, vol. 236, no. 5, pp. 893-906, Apr. 2022.
- [78] J. Shangguan, M. Yue, C. Xu, and J. Zhao, "Robust fault-tolerant estimation of sideslip and roll angles for distributed drive electric buses with stochastic passenger mass," *IEEE Trans. Intell. Transp. Syst.*, vol. 24, no. 12, pp. 14480-14489, Dec. 2023.
- [79] Y. Song, H. Shu, and X. Chen, "Chassis integrated control for 4WIS distributed drive EVs with model predictive control based on the UKF observer," *Sci. China Technol. Sci.*, vol. 63, no. 3, pp. 397-409, Mar. 2020.
- [80] Q. Wang, Y. Zhao, W. Xie, Q. Zhao, and F. Lin, "Hierarchical estimation of vehicle state and tire forces for distributed in-wheel motor drive electric vehicle without previously established tire model," *J. Franklin Inst.*, vol. 359, no. 13, pp. 7051-7068, Sep. 2022.
- [81] B. Leng, C. Tian, X. Hou, L. Xiong, W. Zhao, and Z. Yu, "Tire-road peak adhesion coefficient estimation based on multisource information assessment," *IEEE Trans. Intell. Vehicles*, vol. 8, no. 7, pp. 3854-3870, Jul. 2023.
- [82] L. Gao et al., "Multi-sensor fusion road friction coefficient estimation during steering with Lyapunov method," *Sensors*, vol. 19, no. 18, p. 3816, Sep. 2019.
- [83] L. Shao, C. Jin, C. Lex, and A. Eichberger, "Robust road friction estimation during vehicle steering," *Vehicle Syst. Dyn.*, vol. 57, no. 4, pp. 493-519, Apr. 2019.
- [84] Y. Feng, H. Chen, H. Zhao, and H. Zhou, "Road tire friction coefficient estimation for four wheel drive electric vehicle based on moving optimal estimation strategy," *Mech. Syst. Signal Process.*, vol. 139, May 2020, Art. no. 106416.
- [85] J. Hu, S. Rakheja, and Y. Zhang, "Real-time estimation of tire-road friction coefficient based on lateral vehicle dynamics," *Proc. Inst. Mech. Eng. D, J. Automobile Eng.*, vol. 234, nos. 10-11, pp. 2444-2457, Sep. 2020.
- [86] A. J. Rodriguez, E. Sanjurjo, R. Pastorino, and M. A. Naya, "State, parameter and input observers based on multibody models and Kalman filters for vehicle dynamics," *Mech. Syst. Signal Process.*, vol. 155, Jun. 2021, Art. no. 107544.
- [87] Z. Qin, L. Chen, M. Hu, and X. Chen, "A lateral and longitudinal dynamics control framework of autonomous vehicles based on multi-parameter joint estimation," *IEEE Trans. Veh. Technol.*, vol. 71, no. 6, pp. 5837-5852, Jun. 2022.
- [88] Y. Wang et al., "An integrated scheme for coefficient estimation of tire-road friction with mass parameter mismatch under complex driving scenarios," *IEEE Trans. Ind. Electron.*, vol. 69, no. 12, pp. 13337-13347, Dec. 2022.
- [89] Y. Wang et al., "A novel fault-tolerant scheme for multi-model ensemble estimation of tire road friction coefficient with missing measurements," *IEEE Trans. Intell. Vehicles*, vol. 9, no. 1, pp. 1066-1078, Jan. 2024.
- [90] X. Chen, S. Li, L. Li, W. Zhao, and S. Cheng, "Longitudinal-lateral-cooperative estimation algorithm for vehicle dynamics states based on adaptive-square-root-cubature-Kalman-filter and similarity-principle," *Mech. Syst. Signal Process.*, vol. 176, Aug. 2022, Art. no. 109162.
- [91] R. Zhang, Y. Feng, P. Shi, L. Zhao, Y. Du, and Y. Liu, "Tire-road friction coefficient estimation for distributed drive electric vehicles using PMSM sensorless control," *IEEE Trans. Veh. Technol.*, vol. 72, no. 7, pp. 8672-8685, Jul. 2023.
- [92] Z. Rongyun, Z. Bin, S. Peicheng, Z. Linfeng, F. Yongle, and L. Yarning, "Estimation of state parameters and road adhesion coefficients for distributed drive electric vehicles based on a strong tracking SCKF," *Proc. Inst. Mech. Eng. D, J. Automobile Eng.*, vol. 238, no. 6, pp. 1571-1588, Jan. 2023.
- [93] R.-Y. Zhang, B. Zhang, P.-C. Shi, Y. Mei, Y.-F. Du, and Y.-L. Feng, "Research on the high-speed collision avoidance method of distributed drive electric vehicles," *IEEE Sensors J.*, vol. 23, no. 14, pp. 15813-15830, Jul. 2023.
- [94] L. Zhang, P. Guo, Z. Wang, and X. Ding, "An enabling tire-road friction estimation method for four-in-wheel-motor-drive electric vehicles," *IEEE Trans. Transport. Electricific.*, vol. 9, no. 3, pp. 3697-3710, Sep. 2023.
- [95] F. Xiao, J. Hu, M. Jia, P. Zhu, and C. Deng, "A novel estimation scheme of tyre-road friction characteristics based on parameter constraints on varied- μ roads," *Measurement*, vol. 194, May 2022, Art. no. 111077.
- [96] C. E. Beal, "Rapid road friction estimation using independent left/right steering torque measurements," *Vehicle Syst. Dyn.*, vol. 58, no. 3, pp. 377-403, Mar. 2020.
- [97] M. Sharifzadeh, A. Senatore, A. Farnam, A. Akbari, and F. Timpone, "A real-time approach to robust identification of tyre-road friction characteristics on mixed- μ roads," *Vehicle Syst. Dyn.*, vol. 57, no. 9, pp. 1338-1362, Sep. 2019.
- [98] E. Ono, Y. Hattori, Y. Muragishi, and K. Koibuchi, "Vehicle dynamics integrated control for four-wheel-distributed steering and four-wheel-distributed traction/braking systems," *Vehicle Syst. Dyn.*, vol. 44, no. 2, pp. 139-151, Feb. 2006.
- [99] O. Nishihara and K. Masahiko, "Estimation of road friction coefficient based on the brush model," *J. Dyn. Syst., Meas., Control*, vol. 133, no. 4, pp. 1-9, Apr. 2011.
- [100] C. E. Beal and S. Brennan, "Friction detection from stationary steering manoeuvres," *Vehicle Syst. Dyn.*, vol. 58, no. 11, pp. 1736-1765, Nov. 2020.
- [101] C. E. Beal and S. Brennan, "Modeling and friction estimation for automotive steering torque at very low speeds," *Vehicle Syst. Dyn.*, vol. 59, no. 3, pp. 458-484, Mar. 2021.
- [102] A. M. Ribeiro, A. Moutinho, A. R. Fioravanti, and E. C. de Paiva, "Estimation of tire-road friction for road vehicles: A time delay neural network approach," *J. Brazilian Soc. Mech. Sci. Eng.*, vol. 42, no. 1, pp. 1-12, Nov. 2019.
- [103] Z. Pu, Z. Cui, S. Wang, Q. Li, and Y. Wang, "Time-aware gated recurrent unit networks for forecasting road surface friction using historical data with missing values," *JET Intell. Transp. Syst.*, vol. 14, no. 4, pp. 213-219, Apr. 2020.
- [104] Z. Pu, C. Liu, X. Shi, Z. Cui, and Y. Wang, "Road surface friction prediction using long short-term memory neural network based on historical data," *J. Intell. Transp. Syst.*, vol. 26, no. 1, pp. 34-45, Jan. 2022.
- [105] K. Berntorp, "Online Bayesian inference and learning of Gaussian-process state-space models," *Automatica*, vol. 129, Apr. 2021, Art. no. 109613.
- [106] V. Mussot, G. Mercere, T. Dairay, V. Arvis, and J. Vayssettes, "Model learning of the tire-road friction slip dependency under standard driving conditions," *Control Eng. Pract.*, vol. 121, Jan. 2022, Art. no. 105048.
- [107] N. Xu, E. Hashemi, Z. Tang, and A. Khajepour, "Data-driven tire capacity estimation with experimental verification," *IEEE Trans. Intell. Transp. Syst.*, vol. 23, no. 11, pp. 21569-21581, Nov. 2022.
- [108] G. Wang, S. Li, G. Feng, and Z. Yang, "Road adhesion coefficient estimation by multi-sensors with LM-MMSOFNN algorithm," *Adv. Mech. Eng.*, vol. 15, no. 6, pp. 1-12, Jun. 2023.
- [109] G. Zhang, X. Wang, L. Li, and X. Zhao, "Tire-road friction estimation for four-wheel independent steering and driving EVs using improved CKF and FNN," *IEEE Trans. Transport. Electricific.*, vol. 10, no. 1, pp. 823-834, Mar. 2023.
- [110] Y. Du, C. Liu, Y. Song, Y. Li, and Y. Shen, "Rapid estimation of road friction for anti-skid autonomous driving," *IEEE Trans. Intell. Transp. Syst.*, vol. 21, no. 6, pp. 2461-2470, Jun. 2020.
- [111] Y. Zhan, J. Q. Li, G. Yang, K. C. P. Wang, and W. Yu, "Friction-ResNets: Deep residual network architecture for pavement skid resistance evaluation," *J. Transp. Eng. B, Pavements*, vol. 146, no. 3, Sep. 2020, Art. no. 04020027.
- [112] C. Tian, D. Jin, B. Leng, and L. Xiong, "Reliable identification of road surface condition considering shadow interference," in *Proc. IEEE Int. Intell. Transp. Syst. Conf. (ITSC)*, Sep. 2021, pp. 251-257.
- [113] C. Tian et al., "Robust identification of road surface condition based on ego-vehicle trajectory reckoning," *Automot. Innov.*, vol. 5, no. 4, pp. 376-387, Nov. 2022.
- [114] T. Zhao, J. He, J. Lv, D. Min, and Y. Wei, "A comprehensive implementation of road surface classification for vehicle driving assistance: Dataset, models, and deployment," *IEEE Trans. Intell. Transp. Syst.*, vol. 24, no. 8, pp. 8361-8370, Aug. 2023.

- [115] F. Liu, Y. Wu, X. Yang, Y. Mo, and Y. Liao, "Identification of winter road friction coefficient based on multi-task distillation attention network," *Pattern Anal. Appl.*, vol. 25, no. 2, pp. 441-449, May 2022.
- [116] K. Cordes, C. Reinders, P. Hindricks, J. Lammers, B. Rosenhahn, and H. Broszio, "RoadSaW: A large-scale dataset for camera-based road surface and wetness estimation," in *Proc. IEEE/CVF Conj. Comput. Vis. Pattern Recognit. Workshops (CVPRW)*, Jun. 2022, pp. 4439-4448.
- [117] G. Yang, A. A. Zhang, K. C. P. Wang, J. Q. Li, W. Liu, and Y. Liu, "Deep-learning based non-contact method for assessing pavement skid resistance using 3D laser imaging technology," *Int. J. Pavement Eng.*, vol. 24, no. 2, pp. 1-10, Jan. 2023.
- [118] A. Espindola and R. Rajamani, "Development of an autonomous measurement system for estimation of snow profile on road surfaces," *IEEE Trans. Veh. Technol.*, vol. 72, no. 9, pp. 11169-11183, Sep. 2023.
- [119] B. Leng, D. Jin, L. Xiong, X. Yang, and Z. Yu, "Estimation of tire-road peak adhesion coefficient for intelligent electric vehicles based on camera and tire dynamics information fusion," *Mech. Syst. Signal Process.*, vol. 150, Mar. 2021, Art. no. 107275.
- [120] C. Tian, B. Leng, X. Hou, L. Xiong, and C. Huang, "Multi-sensor fusion based estimation of tire-road peak adhesion coefficient considering model uncertainty," *Remote Sens.*, vol. 14, no. 21, p. 5583, Nov. 2022.
- [121] B. Leng, D. Jin, X. Hou, C. Tian, L. Xiong, and Z. Yu, "Tire-road peak adhesion coefficient estimation method based on fusion of vehicle dynamics and machine vision," *IEEE Trans. Intell. Transp. Syst.*, vol. 23, no. 11, pp. 21740-21752, Nov. 2022.
- [122] Z. Du, A. Skar, M. Pettinari, and X. Zhu, "Pavement friction evaluation based on vehicle dynamics and vision data using a multi-feature fusion network," *Transp. Res. Rec., J. Transp. Res. Board*, vol. 2677, no. 11, pp. 219-236, Apr. 2023.
- [123] H. Guo, X. Zhao, J. Liu, Q. Dai, H. Liu, and H. Chen, "A fusion estimation of the peak tire-road friction coefficient based on road images and dynamic information," *Mech. Syst. Signal Process.*, vol. 189, Apr. 2023, Art. no. 110029.
- [124] L. Gao et al., "Boxes-based representation and data sharing of road surface friction for CAVs," *Data Sci. Transp.*, vol. 5, no. 2, pp. 1-15, Jun. 2023.
- [125] J.-P. Langstrand and M. Rabi, "Estimating road friction from kinematic summaries at curved sections," in *Proc. IEEE Conj. Control Technol. Appl. (CCTA)*, Aug. 2023, pp. 307-314.
- [126] G. Panahandeh, E. Ek, and N. Mohammadiha, "Road friction estimation for connected vehicles using supervised machine learning," in *Proc. IEEE Intell. Vehicles Symp. (IV)*, Jun. 2017, pp. 1262-1267.
- [127] C. Li, P. Liu, Z. Xie, Z. Li, and H. Huan, "Road adhesion coefficient estimation based on vehicle-road coordination and deep learning," *J. Adv. Transp.*, vol. 2023, pp. 1-11, May 2023.
- [128] A. R. Siems-Anderson, C. L. Walker, G. Wiener, W. P. Mahoney, and S. E. Haupt, "An adaptive big data weather system for surface transportation," *Transp. Res. Interdiscipl. Perspect.*, vol. 3, Dec. 2019, Art. no. 100071.
- [129] K. Jiang, D. Yang, S. Xie, Z. Xiao, A. C. Victorino, and A. Charara, "Real-time estimation and prediction of tire forces using digital map for driving risk assessment," *Transp. Res. C, Emerg. Technol.*, vol. 107, pp. 463-489, Oct. 2019.
- [130] J. Hu, M.-C. Huang, and X. B. Yu, "Deep learning based on connected vehicles for icing pavement detection," *AI Civil Eng.*, vol. 2, no. 1, pp. 1-14, Apr. 2023.
- [131] Y. Sun, L. Li, B. Yan, C. Yang, and G. Tang, "A hybrid algorithm combining EKF and RLS in synchronous estimation of road grade and vehicle's mass for a hybrid electric bus," *Mech. Syst. Signal Process.*, vols. 68-69, pp. 416-430, Feb. 2016.
- [132] G. Park and S. B. Choi, "An integrated observer for real-time estimation of vehicle center of gravity height," *IEEE Trans. Intell. Transp. Syst.*, vol. 22, no. 9, pp. 5660-5671, Sep. 2021.
- [133] Z. Zhang, G. Yin, and Z. Wu, "Joint estimation of mass and center of gravity position for distributed drive electric vehicles using dual robust embedded cubature Kalman filter," *Sensors*, vol. 22, no. 24, p. 10018, Dec. 2022.
- [134] Q. Xu, R. Fu, F. Wu, and B. Wang, "Roadside estimation of a vehicle's center of gravity height based on an improved single-stage detection algorithm and regression prediction technology," *IEEE Sensors J.*, vol. 21, no. 21, pp. 24520-24530, Nov. 2021.
- [135] R. A. Cordeiro, A. C. Victorino, J. R. Azinheira, P. A. V. Ferreira, E. C. de Paiva, and S. S. Bueno, "Estimation of vertical, lateral, and longitudinal tire forces in four-wheel vehicles using a delayed interconnected cascade-observer structure," *IEEE/ASME Trans. Mechatronics*, vol. 24, no. 2, pp. 561-571, Apr. 2019.
- [136] X. Ding, Z. Wang, L. Zhang, and J. Liu, "A comprehensive vehicle stability assessment system based on enabling tire force estimation," *IEEE Trans. Veh. Technol.*, vol. 71, no. 11, pp. 11571-11588, Nov. 2022.
- [137] A. H. Salari, H. Mirzaeinejad, and M. F. Mahani, "Tire normal force estimation using artificial neural networks and fuzzy classifiers: Experimental validation," *Appl. Soft Comput.*, vol. 132, Jan. 2023, Art. no. 109835.
- [138] G. Liang et al., "Experimental study of road identification by LSTM with application to adaptive suspension damping control," *Mech. Syst. Signal Process.*, vol. 177, Sep. 2022, Art. no. 109197.
- [139] R. Fan, U. Ozgunalp, Y. Wang, M. Liu, and I. Pitas, "Rethinking road surface 3-D reconstruction and pothole detection: From perspective transformation to disparity map segmentation," *IEEE Trans. Cybern.*, vol. 52, no. 7, pp. 5799-5808, Jul. 2022.
- [140] A. Ahmed, M. Ashfaque, M. U. Ulhaq, S. Mathavan, K. Kamal, and M. Rahman, "Pothole 3D reconstruction with a novel imaging system and structure from motion techniques," *IEEE Trans. Intell. Transp. Syst.*, vol. 23, no. 5, pp. 4685-4694, May 2022.
- [141] J. Yu et al., "Road surface defect detection-From image-based to non-image-based: A survey," *IEEE Trans. Intell. Transp. Syst.*, vol. 25, no. 9, pp. 10581-10603, Apr. 2024.
- [142] H. Chen, M. Yao, and Q. Gu, "Pothole detection using location-aware convolutional neural networks," *Int. J. Mach. Learn. Cybern.*, vol. 11, no. 4, pp. 899-911, 2020.
- [143] A. Dhiman and R. Klette, "Pothole detection using computer vision and learning," *IEEE Trans. Intell. Transp. Syst.*, vol. 21, no. 8, pp. 3536-3550, Aug. 2020.
- [144] J. J. Yebes, D. Montero, and I. Arriola, "Learning to automatically catch potholes in worldwide road scene images," *IEEE Intell. Transp. Syst. Mag.*, vol. 13, no. 3, pp. 192-205, Fall 2021.
- [145] R. Fan, H. Wang, Y. Wang, M. Liu, and I. Pitas, "Graph attention layer evolves semantic segmentation for road pothole detection: A benchmark and algorithms," *IEEE Trans. Image Process.*, vol. 30, pp. 8144-8154, 2021.
- [146] Q. Xie, X. Hu, L. Ren, L. Qi, and Z. Sun, "A binocular vision application in IoT: Realtime trustworthy road condition detection system in passable area," *IEEE Trans. Ind. Informal.*, vol. 19, no. 1, pp. 973-983, Jan. 2023.
- [147] T. Zhao, P. Guo, J. He, and Y. Wei, "A hierarchical scheme of road unevenness perception with LiDAR for autonomous driving comfort," *IEEE Trans. Intell. Vehicles*, vol. 9, no. 1, pp. 2439-2448, Jan. 2024.
- [148] V. Mazzilli et al., "On the benefit of smart tyre technology on vehicle state estimation," *Vehicle Syst. Dyn.*, vol. 60, no. 11, pp. 3694-3719, Nov. 2022.
- [149] S. Sivaramakrishnan, K. B. Singh, and P. Lee, "Influence of tire operating conditions on ABS performance," *Tire Sci. Technol.*, vol. 43, no. 3, pp. 216-241, Sep. 2015.
- [150] K. B. Singh and S. Taheri, "Accelerometer based method for tire load and slip angle estimation," *Vibration*, vol. 2, no. 2, pp. 174-186, Jun. 2019.
- [151] A. Kunnapillil Madhusudhanan, M. Como, M. A. Arat, and E. Holweg, "Load sensing bearing based road-tire friction estimation considering combined tyre slip," *Mechatronics*, vol. 39, pp. 136-146, Nov. 2016.
- [152] A. Bertipaglia, M. Alirezai, R. Happel, and B. Shyrokau, "An unscented Kalman filter-informed neural network for vehicle sideslip angle estimation," *IEEE Trans. Veh. Technol.*, vol. 73, no. 9, pp. 12731-12746, Sep. 2024.
- [153] C. Linguo, P. Haojie, S. Wei, and C. Baigen, "Method of multi-lane vehicles speed continuously perceiving based on single roadside camera," in *Proc. IEEE 25th Int. Conj. Intell. Transp. Syst. (ITSC)*, Oct. 2022, pp. 4314-4319.
- [154] J. Cao, J. Pang, X. Weng, R. Khirodkar, and K. Kitani, "Observation-centric SORT: Rethinking SORT for robust multi-object tracking," in *Proc. IEEE/CVF Conj. Comput. Vis. Pattern Recognit. (CVPR)*, Jun. 2023, pp. 9686-9696.
- [155] W. Jeon, A. Zemouche, and R. Rajamani, "Tracking of vehicle motion on highways and urban roads using a nonlinear observer," *IEEE/ASME Trans. Mechatronics*, vol. 24, no. 2, pp. 644-655, Apr. 2019.
- [156] V. Kumar, S. C. Subramanian, and R. Rajamani, "Vehicle tracking for heavy road vehicle collision avoidance with an inexpensive solid state laser sensor," in *Proc. IEEE Intell. Transp. Syst. Conj. (ITSC)*, Oct. 2019, pp. 1136-1141.
- [157] R. Rajamani, W. Jeon, H. Movahedi, and A. Zemouche, "Vehicle motion estimation using a switched gain nonlinear observer," in *Proc. Amer. Control Conj. (ACC)*, Jul. 2020, pp. 3047-3052.

- [158] H. Bessafa, C. Delattre, Z. Belkhatir, A. Zemouche, and R. Rajamani, "Nonlinear observer design methods based on high-gain methodology and LMIs with application to vehicle tracking," in *Proc. Amer. Control Conf. (ACC)*, May 2023, pp. 4735-4740.
- [159] Z. Zhou, G. Zhou, Y. Wang, H. Du, J.-S. Hu, and C. Yin, "PTV longitudinal-lateral state estimation considering unknown control inputs and uncertain model parameters," *IEEE Trans. Veh. Technol.*, vol. 70, no. 5, pp. 4366-4376, May 2021.
- [160] H. Liu, P. Wang, J. Lin, H. Ding, H. Chen, and F. Xu, "Real-time longitudinal and lateral state estimation of preceding vehicle based on moving horizon estimation," *IEEE Trans. Veh. Technol.*, vol. 70, no. 9, pp. 8755-8768, Sep. 2021.
- [161] Q. Wang, J. Chen, J. Deng, X. Zhang, and K. Zhang, "Simultaneous pose estimation and velocity estimation of an ego vehicle and moving obstacles using LiDAR information only," *IEEE Trans. Intell. Transp. Syst.*, vol. 23, no. 8, pp. 12121-12132, Aug. 2022.
- [162] D. Song, R. Tharmarasa, W. Zhao, G. Li, R. Lee, and T. Kirubarajan, "L-shape model based vehicle tracking with joint kinematic and geometric estimation using lidar," *IEEE Trans. Aerosp. Electron. Syst.*, vol. 59, no. 5, pp. 5768-5777, Oct. 2023.
- [163] H. Lu, P. Wang, X. Fu, H. Chen, and Y. Hu, "A first-order generalized pseudo-Bayesian method based on moving horizon estimation for surrounding vehicle states estimation in complex environments," *Measurement*, vol. 213, May 2023, Art. no. 112678.
- [164] D. Song, R. Tharmarasa, M. C. Florea, N. Duclos-Hindie, X. N. Fernando, and T. Kirubarajan, "Multi-vehicle tracking with microscopic traffic flow model-based particle filtering," *Automatica*, vol. 105, pp. 28-35, Jul. 2019.
- [165] D. Song, R. Tharmarasa, G. Zhou, M. C. Florea, N. Duclos-Hindie, and T. Kirubarajan, "Multi-vehicle tracking using microscopic traffic models," *IEEE Trans. Intell. Transp. Syst.*, vol. 20, no. 1, pp. 149-161, Jan. 2019.
- [166] Z. Tian, Y. Li, M. Cen, and H. Zhu, "Multi-vehicle tracking using an environment interaction potential force model," *IEEE Sensors J.*, vol. 20, no. 20, pp. 12282-12294, Oct. 2020.
- [167] M. B. Khalkhali, A. Vahedian, and H. S. Yazdi, "Multi-target state estimation using interactive Kalman filter for multi-vehicle tracking," *IEEE Trans. Intell. Transp. Syst.*, vol. 21, no. 3, pp. 1131-1144, Mar. 2020.
- [168] M. B. Khalkhali, A. Vahedian, and H. S. Yazdi, "Situation assessment-augmented interactive Kalman filter for multi-vehicle tracking," *IEEE Trans. Intell. Transp. Syst.*, vol. 23, no. 4, pp. 3766-3776, Apr. 2022.
- [169] Y. Wang, Z. Zhou, C. Wei, Y. Liu, and C. Yin, "Host-target vehicle model-based lateral state estimation for preceding target vehicles considering measurement delay," *IEEE Trans. Ind. Informal.*, vol. 14, no. 9, pp. 4190-4199, Sep. 2018.
- [170] J. Hayakawa and B. Dariush, "Ego-motion and surrounding vehicle state estimation using a monocular camera," in *Proc. IEEE Intell. Vehicles Symp. (IV)*, Jun. 2019, pp. 2550-2556.
- [171] Z. Song, J. Lu, T. Zhang, and H. Li, "End-to-end learning for inter-vehicle distance and relative velocity estimation in ADAS with a monocular camera," in *Proc. IEEE Int. Conf. Robot. Autom. (ICRA)*, May 2020, pp. 11081-11087.
- [172] D. K. Jain, R. Jain, L. Cai, M. Gupta, and Y. Upadhyay, "Relative vehicle velocity estimation using monocular video stream," in *Proc. Int. Joint Conf. Neural Netw. (IJCNN)*, Jul. 2020, pp. 1-8.
- [173] H. Fu, J. Guan, F. Jing, C. Wang, and H. Ma, "A real-time multi-vehicle tracking framework in intelligent vehicular networks," *China Commun.*, vol. 18, no. 6, pp. 89-99, Jun. 2021.
- [174] C. Li, Y. Wang, Z. Zhou, J. Wu, W. Jin, and C. Yin, "Lateral state estimation of preceding target vehicle based on multiple neural network ensemble," in *Proc. IEEE Intell. Vehicles Symp. (IV)*, Jun. 2019, pp. 640-646.
- [175] P. Wu, S. Chen, and D. N. Metaxas, "MotionNet: Joint perception and motion prediction for autonomous driving based on bird's eye view maps," in *Proc. IEEE/CVF Conf. Comput. Vis. Pattern Recognit. (CVPR)*, Jun. 2020, pp. 11382-11392.
- [176] X. Chen, J. Ji, and Y. Wang, "Robust cooperative multi-vehicle tracking with inaccurate self-localization based on on-board sensors and inter-vehicle communication," *Sensors*, vol. 20, no. 11, p. 3212, Jun. 2020.
- [177] S. Li, D. Duan, J. Zhang, X. Cheng, and L. Yang, "An efficient distributed multivehicle cooperative tracking framework via multicast," *IEEE Internet Things J.*, vol. 11, no. 1, pp. 158-173, Jan. 2024.
- [178] H. Liu, C. Lin, B. Gong, and H. Liu, "Lane-level and full-cycle multivehicle tracking using low-channel roadside LiDAR," *IEEE Trans. Instrum. Meas.*, vol. 72, pp. 1-12, 2023.
- [179] Z. Zhou, Y. Wang, H. Du, Q. Ji, J.-S. Hu, and C. Yin, "Sub-full model-based heterogeneous sensor fusion for lateral state estimation of preceding target vehicles," *IEEE/ASME Trans. Mechatronics*, vol. 25, no. 3, pp. 1335-1345, Jun. 2020.
- [180] W. Schinkel, T. van der Sande, and H. Nijmeijer, "State estimation for cooperative lateral vehicle following using vehicle-to-vehicle communication," *Electronics*, vol. 10, no. 6, p. 651, Mar. 2021.
- [181] Y. Wang et al., "An event-triggered scheme for state estimation of preceding vehicles under connected vehicle environment," *IEEE Trans. Intell. Veh.*, vol. 8, no. 1, pp. 583-593, Jan. 2023.
- [182] Y. Wang, Z. Hu, S. Lou, and C. Lv, "Interacting multiple model-based ETUKF for efficient state estimation of connected vehicles with V2V communication," *Green Energy Intell. Transp.*, vol. 2, no. 1, Feb. 2023, Art. no. 100044.
- [183] F. Tian, J. Wang, and K. Li, "A novel strong tracking ETUKF for state estimation of preceding vehicles using V2V communications," *IEEE Trans. Veh. Technol.*, vol. 72, no. 10, pp. 12500-12507, Oct. 2023.
- [184] J. Zhao, H. Xu, H. Liu, J. Wu, Y. Zheng, and D. Wu, "Detection and tracking of pedestrians and vehicles using roadside LiDAR sensors," *Transp. Res. C, Emerg. Technol.*, vol. 100, pp. 68-87, Mar. 2019.
- [185] X. Peng and J. Shan, "Detection and tracking of pedestrians using Doppler LiDAR," *Remote Sens.*, vol. 13, no. 15, p. 2952, Jul. 2021.
- [186] Z. Wang, M. Li, Y. Lu, Y. Bao, Z. Li, and J. Zhao, "Effective multiple pedestrian tracking system in video surveillance with monocular stationary camera," *Expert Syst. Appl.*, vol. 178, Sep. 2021, Art. no. 114992.
- [187] H. Wang, L. Jin, Y. He, Z. Huo, G. Wang, and X. Sun, "Detector-tracker integration framework for autonomous vehicles pedestrian tracking," *Remote Sens.*, vol. 15, no. 8, p. 2088, Apr. 2023.
- [188] P. Held, D. Steinhauser, A. Koch, T. Brandmeier, and U. T. Schwarz, "A novel approach for model-based pedestrian tracking using automotive radar," *IEEE Trans. Intell. Transp. Syst.*, vol. 23, no. 7, pp. 7082-7095, Jul. 2022.
- [189] X. Chen, J. Liu, J. Wu, C. Wang, and R. Song, "LoPF: An online LiDAR-only person-following framework," *IEEE Trans. Instrum. Meas.*, vol. 71, pp. 1-13, 2022.
- [190] J. Zhang, W. Xiao, and J. P. Mills, "Optimizing moving object trajectories from roadside LiDAR data by joint detection and tracking," *Remote Sens.*, vol. 14, no. 9, p. 2124, Apr. 2022.
- [191] M. Dimitrievski, P. Veelaert, and W. Philips, "Behavioral pedestrian tracking using a camera and LiDAR sensors on a moving vehicle," *Sensors*, vol. 19, no. 2, p. 391, Jan. 2019.
- [192] X. Fang, J. Li, Z. Zhang, and G. Xiao, "FMCW-MIMO radar-based pedestrian trajectory tracking under Low-observable environments," *IEEE Sensors J.*, vol. 22, no. 20, pp. 19675-19687, Oct. 2022.
- [193] Z. Zhang, X. Wang, D. Huang, X. Fang, M. Zhou, and Y. Zhang, "MRPT: Millimeter-wave radar-based pedestrian trajectory tracking for autonomous urban driving," *IEEE Trans. Instrum. Meas.*, vol. 71, pp. 1-17, 2022.
- [194] Z. Zhang, X. Wang, D. Huang, X. Fang, M. Zhou, and B. Mi, "IDT: An integration of detection and tracking toward low-observable multi-pedestrian for urban autonomous driving," *IEEE Trans. Ind. Informal.*, vol. 19, no. 9, pp. 9887-9897, Sep. 2023.
- [195] Y. Liu, W. Zhang, G. Cui, and Y. Zhang, "Multipedestrian online tracking based on social force-predicted deformable key-points mapping via compressive sensing," *IEEE Syst. J.*, vol. 15, no. 2, pp. 1905-1916, Jun. 2021.
- [196] K.-I. Na, S. Choi, and J.-H. Kim, "Adaptive target tracking with interacting heterogeneous motion models," *IEEE Trans. Intell. Transp. Syst.*, vol. 23, no. 11, pp. 21301-21313, Nov. 2022.
- [197] Y. Zhu, T. Wang, and S. Zhu, "Adaptive multi-pedestrian tracking by multi-sensor: Track-to-track fusion using monocular 3D detection and MMW radar," *Remote Sens.*, vol. 14, no. 8, p. 1837, Apr. 2022.
- [198] F. Cui et al., "Online multipedestrian tracking based on fused detections of millimeter wave radar and vision," *IEEE Sensors J.*, vol. 23, no. 14, pp. 15702-15712, Jul. 2023.
- [199] L. Wang et al., "CAMO-MOT: Combined appearance-motion optimization for 3D multi-object tracking with camera-LiDAR fusion," *IEEE Trans. Intell. Transp. Syst.*, vol. 24, no. 11, pp. 11981-11996, Nov. 2023.
- [200] M. Gao, L. Jin, Y. Jiang, and J. Bie, "Multiple object tracking using a dual-attention network for autonomous driving," *JET Intell. Transp. Syst.*, vol. 14, no. 8, pp. 842-848, Aug. 2020.
- [201] J. Che, Y. He, and J. Wu, "Pedestrian multiple-object tracking based on FairMOT and circle loss," *Sci. Rep.*, vol. 13, no. 1, pp. 1-12, Mar. 2023.

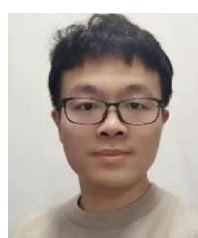
- [202] G. Li et al., "Pedestrian tracking based on receptive field improvement: A one-shot multiobject tracking approach based on vision sensors," *IEEE Sensors J.*, vol. 23, no. 16, pp. 18893-18907, Aug. 2023.
- [203] F. Xie, C. Wang, G. Wang, W. Yang, and W. Zeng, "Learning tracking representations via dual-branch fully transformer networks," in *Proc. IEEE/CVF Int. Conj. Comput. Vis. Workshops (ICCVW)*, Oct. 2021, pp. 2688-2697.
- [204] Y. Liu et al., "SegDQ: Segmentation assisted multi-object tracking with dynamic query-based transformers," *Neurocomputing*, vol. 481, pp. 91-101, Apr. 2022.
- [205] Y. Xu, Y. Ban, G. Delorme, C. Gan, D. Rus, and X. Alameda-Pineda, "TransCenter: Transformers with dense representations for multiple-object tracking," *IEEE Trans. Pattern Anal. Mach. Intel.*, vol. 45, no. 6, pp. 7820-7835, Jun. 2023.
- [206] P. Nguyen, K. G. Quach, C. N. Duong, N. Le, X.-B. Nguyen, and K. Luu, "Multi-camera multiple 3D object tracking on the move for autonomous vehicles," in *Proc. IEEE/CVF Conj. Comput. Vis. Pattern Recognit. Workshops (CVPRW)*, Jun. 2022, pp. 2568-2577.
- [207] T. Meinhardt, A. Kirillov, L. Leal-Taixe, and C. Feichtenhofer, "TrackFormer: Multi-object tracking with transformers," in *Proc. IEEE/CVF Conj. Comput. Vis. Pattern Recognit. (CVPR)*, Jun. 2022, pp. 8834-8844.
- [208] P. Chu, J. Wang, Q. You, H. Ling, and Z. Liu, "TransMOT: Spatial-temporal graph transformer for multiple object tracking," in *Proc. IEEE/CVF Winter Conj. Appl. Comput. Vis. (WACV)*, Jan. 2023, pp. 4859-4869.
- [209] T. Zhu et al., "Looking beyond two frames: End-to-end multi-object tracking using spatial and temporal transformers," *IEEE Trans. Pattern Anal. Mach. Intel.*, vol. 45, no. 11, pp. 12783-12797, Nov. 2023.
- [210] S. Ding, E. Rehder, L. Schneider, M. Cordts, and J. Gall, "3DMOT-Former: Graph transformer for online 3D multi-object tracking," in *Proc. IEEE/CVF Int. Conj. Comput. Vis. (ICCV)*, Oct. 2023, pp. 9750-9760.
- [211] X. Chen et al., "TrajectoryFormer: 3D object tracking transformer with predictive trajectory hypotheses," in *Proc. IEEE/CVF Int. Conj. Comput. Vis. (ICCV)*, Oct. 2023, pp. 18481-18490.
- [212] H. Liu, Y. Ma, H. Wang, C. Zhang, and Y. Guo, "AnchorPoint: Query design for transformer-based 3D object detection and tracking," *IEEE Trans. Intel. Transp. Syst.*, vol. 24, no. 10, pp. 10988-11000, Oct. 2023.
- [213] C. Zhang, C. Zhang, Y. Guo, L. Chen, and M. Happold, "MotionTrack: End-to-end transformer-based multi-object tracking with LiDAR-camera fusion," in *Proc. IEEE/CVF Conj. Comput. Vis. Pattern Recognit. Workshops (CVPRW)*, Jun. 2023, pp. 151-160.
- [214] V. M. Scarrica, C. Panariello, A. Ferone, and A. Staiano, "A hybrid approach to real-time multi-target tracking," *Neural Comput. Appl.*, vol. 36, no. 17, pp. 10055-10066, Jun. 2024.
- [215] J. Li, H. Ma, Z. Zhang, J. Li, and M. Tomizuka, "Spatio-temporal graph dual-attention network for multi-agent prediction and tracking," *IEEE Trans. Intel. Transp. Syst.*, vol. 23, no. 8, pp. 10556-10569, Aug. 2022.
- [216] A. Geiger, P. Lenz, and R. Urtasun, "Are we ready for autonomous driving? The KITTI vision benchmark suite," in *Proc. IEEE Conj. Comput. Vis. Pattern Recognit.*, Jun. 2012, pp. 3354-3361.
- [217] F. Yu et al., "BDD100K: A diverse driving dataset for heterogeneous multitask learning," in *Proc. IEEE/CVF Conj. Comput. Vis. Pattern Recognit. (CVPR)*, Jun. 2020, pp. 2633-2642.
- [218] P. Dendorfer et al., "MOT20: A benchmark for multi object tracking in crowded scenes," 2020, *arXiv:2003.09003*.
- [219] H. Caesar et al., "nuScenes: A multimodal dataset for autonomous driving," in *Proc. IEEE/CVF Conj. Comput. Vis. Pattern Recognit. (CVPR)*, Jun. 2020, pp. 11618-11628.
- [220] T. Zhao, Y. Xie, M. Ding, L. Yang, M. Tomizuka, and Y. Wei, "A road surface reconstruction dataset for autonomous driving," *Sci. Data*, vol. 11, no. 1, pp. 459-469, May 2024.
- [221] X. Li, L. Guvenc, and B. Aksun-Guvenc, "Vehicle state estimation and prediction for autonomous driving in a round intersection," *Vehicles*, vol. 5, no. 4, pp. 1328-1352, Oct. 2023.
- [222] D. Deter, C. Wang, A. Cook, and N. K. Perry, "Simulating the autonomous future: A look at virtual vehicle environments and how to validate simulation using public data sets," *IEEE Signal Process. Mag.*, vol. 38, no. 1, pp. 111-121, Jan. 2021.
- [223] A. Dosovitskiy, G. Ros, F. Codevilla, A. Lopez, and V. Koltun, "CARLA: An open urban driving simulator," in *Proc. Annu. Conj. Robot. Learn. (CoRL)*, vol. 78, Nov. 2017, pp. 1-16.
- [224] A.-T. Nguyen, L. Frezzatto, T.-M. Guerra, and S. Delprat, "Cost-effective estimation of vehicle lateral tire-road forces and sideslip angle via nonlinear sampled-data observers: Theory and experiments," *IEEE/ASME Trans. Mechatronics*, early access, Apr. 17, 2024, doi: 10.1109/TMECH.2024.3382777.
- [225] Z. Ju, H. Zhang, X. Li, X. Chen, J. Han, and M. Yang, "A survey on attack detection and resilience for connected and automated vehicles: From vehicle dynamics and control perspective," *IEEE Trans. Intel. Vehicles*, vol. 7, no. 4, pp. 815-837, Dec. 2022.
- [226] X. Sun, F. R. Yu, and P. Zhang, "A survey on cyber-security of connected and autonomous vehicles (CAVs)," *IEEE Trans. Intel. Transp. Syst.*, vol. 23, no. 7, pp. 6240-6259, Jul. 2022.
- [227] S. Feng et al., "Dense reinforcement learning for safety validation of autonomous vehicles," *Nature*, vol. 615, no. 7953, pp. 620-627, Mar. 2023.
- [228] S. Yang, Y. Chen, R. Shi, R. Wang, Y. Cao, and J. Lu, "A survey of intelligent tires for tire-road interaction recognition toward autonomous vehicles," *IEEE Trans. Intel. Vehicles*, vol. 7, no. 3, pp. 520-532, Sep. 2022.
- [229] H. Lin, Y. Liu, S. Li, and X. Qu, "How generative adversarial networks promote the development of intelligent transportation systems: A survey," *IEEE/CAA J. Autom. Sinica*, vol. 10, no. 9, pp. 1781-1796, Sep. 2023.
- [230] V. Bharilya and N. Kumar, "Machine learning for autonomous vehicle's trajectory prediction: A comprehensive survey, challenges, and future research directions," *Veh. Commun.*, vol. 46, Jan. 2024, Art. no. 100733.



Cheng Tian (Graduate Student Member, IEEE) received the M.Eng. degree in vehicle engineering from Tongji University, Shanghai, China, in 2022. He is currently pursuing the Ph.D. degree with the Department of Aeronautical and Aviation Engineering, The Hong Kong Polytechnic University, Hong Kong, SAR, China. His research interests include vehicle dynamics and control, safe planning, and control for autonomous vehicles.



Chao Huang (Senior Member, IEEE) is currently a Research Assistant Professor with the Department of Industrial and System Engineering, The Hong Kong Polytechnic University (PolyU). Her research interests include human-machine collaboration, fault-tolerant control, mobile robots (EV, UAV), and path planning and control. She serves as an Associate Editor for IEEE TRANSACTIONS ON TRANSPORTATION ELECTRIFICATION, Engineering Applications of Artificial Intelligence, IEEE TRANSACTIONS ON CONSUMER ELECTRONICS, and Control Engineering Practice.



Yan Wang (Member, IEEE) received the Ph.D. degree in mechanical engineering from Southeast University, Nanjing, China, in 2022. He was a Research Fellow with Nanyang Technological University. He is currently a Research Associate with The Hong Kong Polytechnic University. His current research interests include vehicle system dynamics and automotive active safety control. He is a Youth Editorial Board Member of Chinese Journal of Mechanical Engineering and Journal of Measurement Science and Instrumentation.



Edward Chung received the bachelor's and Ph.D. degrees from Monash University. He is currently a Professor of intelligent transport systems with The Hong Kong Polytechnic University (PolyU). Prior to his appointment at PolyU, he was a Professor and the Director of the Smart Transport Research Centre, Queensland University of Technology. He has many years of experience as an experienced Academician and a Researcher, working both domestically and internationally. His research interests include connected autonomous vehicles, artificial intelligence, traffic management, and transport modeling.



Anh-Tu Nguyen (Senior Member, IEEE) received the Diplôme d'Ingenieur and M.Sc. degrees in automatic control from Grenoble Institute of Technology, Grenoble, France, in 2009, and the Ph.D. degree in automatic control from the University of Valenciennes, Valenciennes, France, in 2013. He is currently an Associate Professor with INSA Hauts-de-France, Université Polytechnique Hauts-de-France, Valenciennes. His research interests include robust control and estimation, cybernetics control systems, and human-machine shared control with a strong emphasis on mechatronics applications.



Pak Kin Wong received the Ph.D. degree in mechanical engineering from The Hong Kong Polytechnic University, Hong Kong, in 1997. He is currently a Professor with the Department of Electromechanical Engineering, University of Macau, Macau, China. He has authored or co-authored more than 350 scientific papers in refereed journals, book chapters, and conference proceedings. His research interests include automotive engineering, fluid transmission and control, mechanical vibration, and artificial intelligence for medical application.



Wei Ni (Fellow, IEEE) received the B.E. and Ph.D. degrees in communication science and engineering from Fudan University, Shanghai, China, in 2000 and 2005, respectively. He is currently a Principal Research Scientist with CSIRO, Sydney, Australia; a Conjoint Professor with the University of New South Wales; an Adjunct Professor with the University of Technology Sydney; and a Honorary Professor with Macquarie University. His research interests include machine learning, online learning, and stochastic optimization, and their applications

to the security, integrity, and efficiency of network systems. He has been an Editor of IEEE TRANSACTIONS ON VEHICULAR TECHNOLOGY since 2022, IEEE TRANSACTIONS ON WIRELESS COMMUNICATIONS since 2018, and *Research Directions: Cyber-Physical Systems* (Cambridge Press New) since 2022.



Abbas Jamalipour (Fellow, IEEE) received the Ph.D. degree in electrical engineering from Nagoya University, Nagoya, Japan, in 1996.

He holds the position of Professor of ubiquitous mobile networking with The University of Sydney. He has authored nine technical books, 11 book chapters, over 550 technical articles, and five patents, all in the area of wireless communications and networking. He is a fellow of the Institute of Electrical, Information, and Communication Engineers (IEICE) and the Institution of Engineers Australia, an ACM Professional Member, and an IEEE Distinguished Speaker. He has been the Editor-in-Chief of IEEE TRANSACTIONS ON VEHICULAR TECHNOLOGY, since January 2022. Previously, he held the positions of Executive Vice-President and Editor-in-Chief of VTS Mobile World and has been an elected member of the Board of Governors of the IEEE Vehicular Technology Society since 2014. He was the Editor-in-Chief of IEEE WIRELESS COMMUNICATIONS, the Vice President-Conferences, and a member of the Board of Governors of the IEEE Communications Society. He sits on the Editorial Board of IEEE ACCESS and several other journals and is a member of the Advisory Board of the IEEE INTERNET OF THINGS JOURNAL. He has been the General Chair or the Technical Program Chair of several prestigious conferences, including IEEE ICC, GLOBECOM, WCNC, and PIMRC.



Kai Li (Senior Member, IEEE) received the B.E. degree from Shandong University, Weihai, China, in 2009, the M.S. degree from The Hong Kong University of Science and Technology, Hong Kong, in 2010, and the Ph.D. degree in computer science from the University of New South Wales, Sydney, NSW, Australia, in 2014. He is currently a Visiting Research Scholar with the School of Electrical Engineering and Computer Science, TU Berlin, Germany, and a Senior Research Scientist with the CISTER Research Centre, Porto, Portugal. He has been an Associate Editor of journals, such as *Internet of Things* (Elsevier) since 2024, *Nature Computer Science* (Springer) since 2023, *Computer Communications* (Elsevier), and *Ad Hoc Networks* (Elsevier) since 2021.



Hailong Huang (Senior Member, IEEE) received the Ph.D. degree in systems and control from the University of New South Wales, Sydney, Australia, in 2018. He is currently an Assistant Professor with the Department of Aeronautical and Aviation Engineering, The Hong Kong Polytechnic University, Hong Kong. His current research interests include guidance, navigation, and control of UAVs and mobile robots.